between the sensitive and resistant cells. Bcl-xL was not detected even by the fractionation experiments (not shown). The localization of trifunctional protein in mitochondria (Kamijo *et al*., 1993) and β-tubulin in the cytosol confirmed the reliability of the fractionation procedures. Importantly, similar results on the Noxa kinetics in mitochondria were observed after the treatment by etoposide, the other p53-dependent damage-inducing anticancer drug in NB cells (Figure 4B). Consistent with the results of WST-8 assay (Figure 1b), Noxa upregulation in mitochondria was observed in etoposide-sensitive SK-N-SH, NB-9 and NB-19 cells but not in IMR32 cells. These results suggest that the ratio of pro- to anti-apoptotic molecules such as Noxa/Bcl-2 has a strong impact on the p53-dependent damage-induced apoptosis in NB cells.

Next, we assessed *Noxa* mRNA amounts in NB tumor samples by semi-quantitative RT–PCR (Figure 4C) and quantitative real-time reverse transcriptional (RT)–PCR (Figure 4D). Consistent with the upregulation of *Noxa* mRNA in the resistant cell lines (Figures 3b and c), some unfavorable NB samples expressed large amounts of *Noxa* mRNA (Figure 4C). Especially, high levels of *Noxa* mRNA expression were significantly associated with INSS3 and INSS4 samples that were younger than 12 months old ($P=0.04$) according to the Welch test (Figure 4D). In the NB samples that were older than 12 months old, no obvious difference was detected, mainly due to the high expression of Noxa in INSS 1 samples. Although we checked the correlation of *MYCN* and *Noxa* mRNA expression, there was no significant correlation (data not shown).

Knockdown of Noxa effectively reduces Doxo-induced cell death in NB cells

To definitively establish a role of Noxa in Doxo-induced cell death in NB cells, both of the sensitive SK-N-SH cells and the resistant IMR32 cells were treated with *Noxa* small interfering RNA (siRNA) and then the NB cells had Doxo administered. Preincubation of the NB cells with the *Noxa* siRNA but not control siRNA effectively reduced the *Noxa* mRNA and also protein amounts in SK-N-SH cells (Figures 5a and b). Since the effectiveness of *Noxa* siRNA1 is better than that of *Noxa* siRNA2, we used *Noxa* siRNA1 for later experiments. The *Noxa* siRNA1 did not affect the pro-apoptotic Bcl-2 family molecules (Bax and Bak), an important inhibitor of apoptosis $p21^{Cip1/Waf1}$ and interferon-α (Figure 5c), suggesting that the knockdown seems to have a specific effect on Noxa. The ability of the *Noxa* siRNA to reduce the *Noxa* mRNA amounts was accompanied by a significant reduction in the

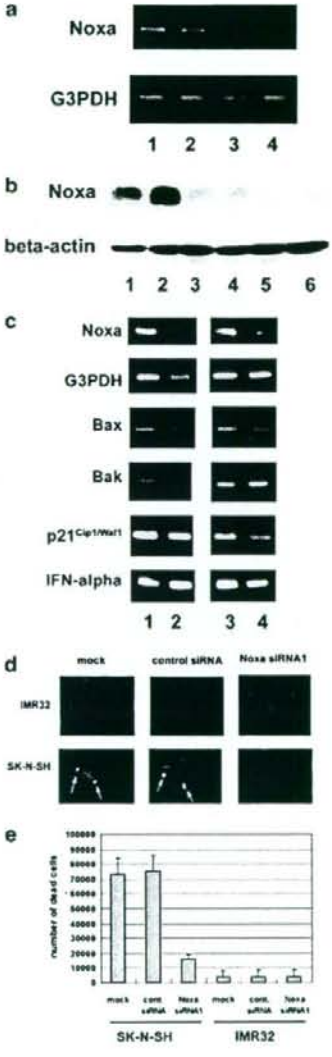

Figure 5 Noxa knockdown cancels Doxo-induced apoptotic cell death in sensitive neuroblastoma (NB) cells. (**a**) SK-N-SH cells were collected 48 h after small interfering RNA (siRNA) treatment (lane 1: mock; lane 2: control siRNA; lane 3: Noxa siRNA1; lane 4: Noxa siRNA2) and subjected to cDNA synthesis/semi-quantitative RT–PCR procedure. (**b**) SK-N-SH cells (lane 3: mock; lane 4: control siRNA; lane 5: Noxa siRNA1; lane 6: Noxa siRNA2) were collected 48 h after siRNA treatment and 30 μg of proteins was subjected to sodium dodecyl sulfate–polyacrylamide gel electrophoresis (SDS–PAGE)/western blot analysis. Lanes 1 and 2 were nontreated IMR32 and NB-19 cells, respectively, as controls. (**c**) Forty-eight hours after the siRNA treatment, cells were treated with 0.5 μg/ml Doxo. Twenty-four hours after Doxo administration, SK-N-SH (lanes 1 and 2) and IMR32 (lanes 3 and 4) cells were collected and subjected to cDNA synthesis/semi-quantitative RT–PCR for the analysis of the molecules indicated at the left side of panel. Lanes 1 and 3 are control siRNA treated, and lanes 2 and 4 are Noxa siRNA1 treated. (**d** and **e**) Forty-eight hours after the siRNA treatment, cells were treated with 0.5 μg/ml Doxo. Twenty-four hours after Doxo administration, the culture dish-attached SK-N-SH and IMR32 cells were stained with 4′,6-diamidino-2-phenylindole (DAPI) and nuclear morphology was analysed. The floating cells were collected and subjected to Trypan blue uptake analysis. Trypan blue-positive cells were counted as 'dead cells.'

apoptotic morphological change of nuclei (nuclear condensation and fragmentation, Figure 5c) and cell death (Figure 5d) in the Doxo-sensitive SK-N-SH cells but not in the resistant IMR32 cells.

Doxo-induced stress induces mitochondrial dysfunction and activates the intrinsic caspase pathway

Next, we evaluated mitochondria homeostasis and activation of caspase pathways in NB cells. First, we investigated the role of mitochondrial membrane potential in Doxo-induced apoptosis. Mitochondrial membrane potential was assessed 10 h after Doxo stimulation by staining with the mitochondrion-selective dye, MitoTracker. Doxo-sensitive cells exhibited substantial mitochondrial depolarization, as evidenced by the loss of MitoTracker staining (Figure 6a). In contrast, depolarization was not induced by Doxo in the resistant cells. Next, immunofluorescence experiments showed that cytochrome-*c* was clearly released from mitochondria in the sensitive cells but not in the resistant cells (Figure 6b, Doxo-treated cells, 'Cyto. C' panels). Nuclear condensation was especially observed in the cells from which large amounts of cytochrome-*c* were released (Doxo-treated cells, 'Nuc' panels). These results suggest that mitochondrial dysfunction plays a pivotal role in Doxo-induced apoptosis in NB cells.

The central component of apoptosis is a proteolytic system involving a family of proteases called caspases (Green, 2000). As shown in Figure 6c, pro-caspase-9 cleavage was observed in the Doxo-sensitive cells, but not in the resistant cells 12 h after exposure to Doxo. The substrates of the activated caspase-9, pro-caspase-3 and -7 were also cleaved in the Doxo-sensitive cells. These findings suggest that apoptotic signals induced by Doxo activate the intrinsic caspase pathway via a mitochondrial pathway in NB cells, resulting in cell death of the Doxo-sensitive NB cells. Meanwhile, the resistant cells showed no activation of these initiator (caspase-9) and effector (caspase-3 and/or -7) caspases.

Discussion

Human *Noxa* is located on chromosome 18q21 and its promoter region contains a p53-responsive element (Oda *et al*., 2003). The expression of p53 increases human *Noxa* mRNA, and ectopic expression of Noxa effectively induces apoptosis in a BH3-motif-dependent manner (Oda *et al*., 2003). In the present study, we observed that Doxo-sensitive NB cells exhibited the Noxa mRNA/protein induction and protein localization into mitochondria after the treatment with Doxo, leading to an increase in the ratio of pro-/anti-apoptotic Bcl-2 family proteins. Mitochondrial dysfunction and intrinsic caspase-mediated apoptosis were also induced in the sensitive cells. Notably, apoptosis was almost completely canceled by the knockdown of Noxa by siRNA, confirming the importance of Noxa in the Doxo-induced apoptosis of NB cells. Taken together, these findings indicate that the Noxa upregulation in mitochondria may play an important role in Doxo-induced apoptosis in NB cells. A previous study described that Noxa and Bok were induced by etoposide, and *Noxa* siRNA treatment reduced etoposide-induced cell death in SH-SY5Y NB cells (Yakovlev *et al*., 2004). Furthermore, Obexer *et al*. (2007) reported that Noxa and Bim are effectors of FKHRL-1-induced apoptosis in NB cells. Since we also observed the upregulation of Noxa in mitochondria by Doxo or etoposide treatment, Noxa seems to be one of the important effectors of the pro-apoptotic signaling pathway in NB cell apoptosis.

Whereas Yakovlev *et al*. (2004) did not use stress-resistant NB cells, the kinetics of Noxa induction in the stress-resistant NB cells was evaluated in our study. In the Doxo-resistant NB cells, exposure to Doxo failed to increase the expression of Noxa and the other downstream molecules in mitochondria, although p53 was abundant in the nucleus before Doxo exposure and some of the p53 serine residues that regulate p53 stability and activity (Shieh *et al*., 1997; Oda *et al*., 2000) were efficiently phosphorylated in the resistant cells, as well as in the sensitive cells. These results suggest that the lack of some p53 function in the resistant NB cells results in the failure of apoptosis, even under the pressure of DNA damage, such as Doxo treatment. It is of interest that the amounts of *Noxa* mRNA and protein in the mitochondria were much larger in the unstimulated resistant cells than in the sensitive cells but not stimulated by Doxo treatment. Alternatively, the inability to upregulate Noxa transcription in response to Doxo may be related to resistance to the anthracycline in some NB cells. Large amounts of *Noxa* mRNA in a part of unfavorable NB primary tumor samples (Figure 4C) supported the observation of inactivity of accumulated Noxa in the resistant cells. The accumulation of Noxa in unstimulated NB cells seems to be p53 independent, as it was suggested by our experiments. Although several findings suggest that Noxa is induced via a p53-independent pathway in neuronal cells (Kiryu-Seo *et al*., 2005; Wong *et al*., 2005), the exact molecular pathway responsible for the p53-independent Noxa induction in NB remains to be elucidated. One possibility is the presence of other p53 family proteins, for example, p63 and p73 proteins in NB cells. Actually, p73-alpha is expressed in several NB cell lines, including IMR32 and NB19 cells, and p63, but not deltaNp63, is highly expressed at the transcriptional level in IMR32 cells (data not shown). The study of the physiological role of p63 and p73 proteins on Noxa expression and Doxo-induced NB cell death seems to be meaningful for research of NB cell death.

A previous report indicated that although Noxa expression mediated by adenovirus could not induce apoptosis in either wild-type or *p53*-knockout MEFs, its expression effectively enhanced the apoptotic response to etoposide or UV (Shibue *et al*., 2003), suggesting that Noxa induces apoptosis in concert with not only p53-dependent cellular signals, but also p53-independent cellular signals. Additionally, we found a significant increase of *Noxa* mRNA amounts in the tumor samples

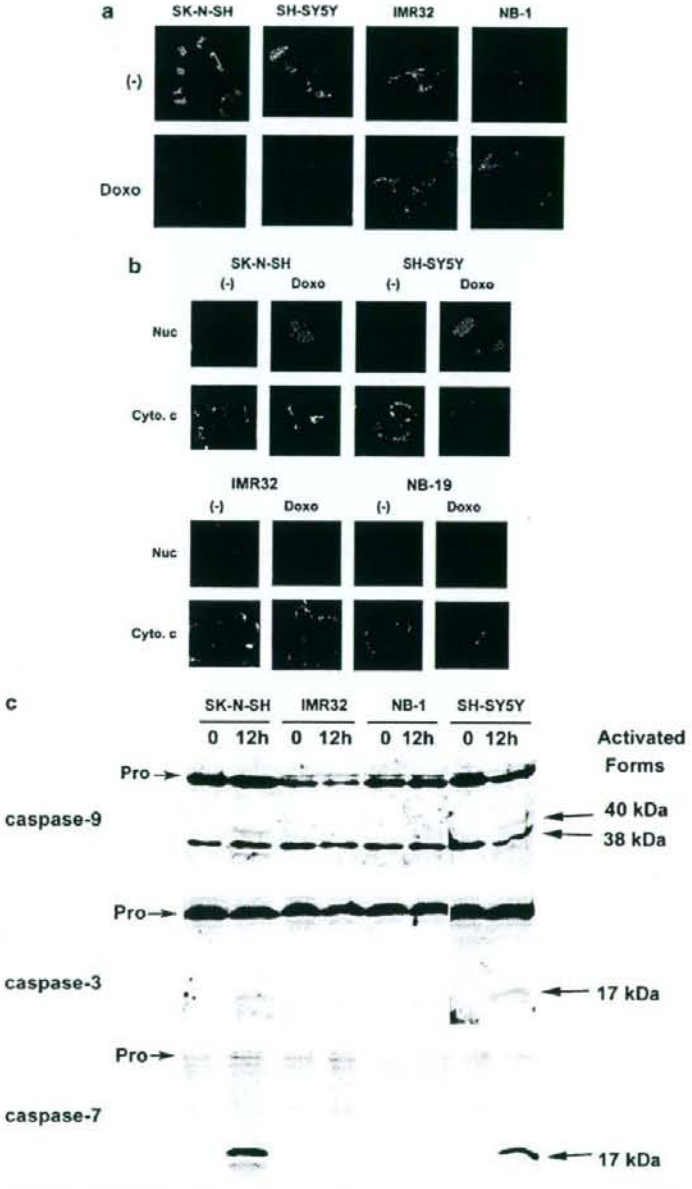

Figure 6 Mitochondrial dysfunction is induced by Doxo in the sensitive neuroblastoma (NB) cells. (**a**) Mitochondrial membrane potential was detected using MitoTracker dye 6 h after Doxo stimulation (Doxo). The steady-state potential is shown as a control [(−)]. (**b**) Cells were stimulated with Doxo for 6 h, and then cytochrome-*c* (Cyto. c) signals were detected by immunofluorescence experiments. The nucleus (Nuc) was stained with 4′,6-diamidino-2-phenylindole (DAPI). (**c**) Cells were collected at the indicated time points after Doxo stimulation and subjected to sodium dodecyl sulfate–polyacrylamide gel electrophoresis (SDS–PAGE)/western blot analysis. Processing of pro-caspase-9 was detected by the presence of 38/40-kDa cleaved forms. The anti-caspase-3 rabbit polyclonal antibody (BD Pharmingen) recognized the 32-kDa pro-caspase-3 and the 17-kDa cleaved form. The anti-caspase-7 mouse monoclonal antibody (clone B94-1) recognized the 35-kDa pro-caspase-7 and the 17-kDa cleaved form.

in the advanced stage (INSS3 and -4, younger than 12 months old) by quantitative real-time RT–PCR analysis (Figure 4D), indicating that the inactiveness of *Noxa* may relate to the progression in NB tumors. These observations suggest that reactivation of the accumulated Noxa in the Doxo-resistant NB cells with p53-independent stress may provide a new therapeutic approach to chemotherapy-resistant NB. Moreover, biochemical analysis of the accumulated Noxa in the mitochondria of resistant cells, for example, the analysis of Noxa-binding Bcl-2-family proteins in mitochondria, may be useful to address the mechanism of the failure of Doxo-induced apoptosis in those cells.

To address the other potential mechanisms of the resistances of DNA-damage-induced reagents in the chosen cell lines, we studied the genomic amplification of *MYCN* (Materials and methods), *caspase-8* and *P-glycoprotein* mRNA expression by semi-quantitative RT–PCR (data not shown). Caspase-8 was expressed in NB-9, NB-69, SK-N-SH and NB-1 cells. However, caspase-8 seems not to have a significant role in the Doxo-induced NB apoptosis, since we could not detect its activation by western blotting (data not shown). P-glycoprotein was clearly expressed in NB-9, NB-69, SK-N-SH and NB-1 cells, but not in SH-SY5Y, NB-1, and IMR32 cells (data not shown), suggesting that p-glycoprotein seems not to relate to the Doxo sensitivity of NB cells. Regarding *MYCN* amplification status, all the three resistant cell lines had *MYCN* amplification and three of four sensitive cell lines had single copy *MYCN*, suggesting that inactivity of p53 in the resistant cell lines may relate to the *MYCN* amplification. Consistent with our observation, Bell *et al.* (2006) reported that *MYCN* amplification correlates with attenuated $p21^{Cip1/Waf1}$ induction in *p53* wild-type NB cells. The analysis of the molecular mechanism between *MYCN* amplification and p53 inactivation in NB cells may be important for NB studies.

Taken together, our findings indicate that the p53 pathway regulates NB cell apoptosis via pro-apoptotic Noxa kinetics and localization in the mitochondria. Further study of Noxa in NB may provide an important approach to develop new therapies for NB and to improve the prognosis of high-risk NB patients.

Materials and methods

Reagents and antibodies

Anti-p53 mouse monoclonal antibody (clone DO-1), anti-Bcl-2 mouse monoclonal antibody (clone C-2), anti-$p21^{Cip1/Waf1}$ mouse monoclonal antibody (clone F-5) and anti-Bad mouse monoclonal antibody (clone C-7) were from Santa Cruz Biotechnology Inc. (Santa Cruz, CA, USA). Anti-cytochrome-*c* mouse monoclonal antibody (clone 7H8.2C12), anti-Bcl-xL mouse monoclonal antibody (clone 2H12), anti-caspase-3 rabbit polyclonal antibody, anti-caspase-7 mouse monoclonal antibody (clone B94-1) and anti-Bid rabbit polyclonal antibody were from BD PharMingen (San Diego, CA, USA). Anti-phospho-p53 rabbit serum (p53ser15p, p53ser20p and p53ser46p) and anti-phospho-p53ser15 mouse monoclonal antibody (clone 16G8) were from Cell Signaling Technology (Beverly, MA, USA). Anti-Bax and Anti-Bak rabbit polyclonal antibodies were from Upstate Biotechnology (Lake Placid, NY, USA). Anti-p53 mouse monoclonal antibody (clone pAb421), anti-p53 sheep polyclonal Antisera (Ab-7) Kit and anti-Noxa mouse monoclonal antibody (clone 114C307, for immunofluorescence analysis) were from Oncogene Research Products (Cambridge, MA, USA). Anti-Noxa rabbit polyclonal antibody (for western blotting) was from Abcam (Cambridge, UK). Anti-Bim rabbit polyclonal antibody was from Millennium Biotechnology (Ramona, CA, USA). Anti-Bok rabbit polyclonal antibody was from ABGENT (San Diego, CA, USA). Anti-caspase-9 mouse monoclonal antibody (clone 5B4) was from MBL (Nagoya, Japan). Anti-lamin monoclonal antibody (clone JOL2) was from Chemicon (Temecula, CA, USA). Anti-β-tubulin mouse monoclonal antibody (clone KMX-1) was from Roche Diagnostics (Manheim, Germany). Anti-trifunctional protein serum was prepared by rabbit immunization and affinity selection with purified trifunctional protein (Kamijo *et al.*, 1993). Anti-HDM2 monoclonal antibody (clone 2A10) was a generous gift from Dr Arnold J Levine, Pediatrics and Biochemistry Cancer Institute of New Jersey. Other biochemical reagents were purchased from Sigma-Aldrich Japan, or Wako (Osaka, Japan).

Cells and cell culture

We collected p53 wild-type NB cell lines to study the role of the p53 pathway in drug resistance mechanism of NB cells. SK-N-SH, NB-9, NB-19 and NB69 were obtained from Riken Cell Bank (Tsukuba, Japan). IMR32 and NB-1 were from Cell Resource Center for Biomedical Research Institute of Development, Aging and Cancer, Tohoku University. The wild-type *p53*-expressing SH-SY5Y line was purchased from ATCC (Manassas, VA, USA). The wild-type p53 status was demonstrated in previous reports (IMR32: Hopkins-Donaldson *et al.*, 2002; SK-N-SH: Wolff *et al.*, 2001) and p53 sequencing, which was performed according to the previous report (Tweddle *et al.*, 2001), confirmed the wild-type p53 status in these cell lines. In terms of the copy number of MYCN by Southern blot analysis, SH-SY5Y, SK-N-SH and NB-69 are single-copy NB cells; NB-9, IMR32, NB-1 and NB-19 cells have 50, >150, >150 and 25 copies, respectively (data not shown). The cells were routinely maintained with DMEM supplemented with 10% fetal bovine serum (FBS) and 1 × penicillin/streptomycin (Invitrogen, Carlsbad, CA, USA).

Tumor samples

Fresh, frozen tumor tissues were sent to the Division of Biochemistry, Chiba Cancer Center Research Institute, from various hospitals in Japan with informed consent from the patients' parents. All samples were obtained by surgery or biopsy and stored at −80°C. More than 70% of tumor cell contents of the samples were confirmed by pathological analysis of the adjacent tissues. Studies were approved by the Institutional Review Board of the Chiba Cancer Center.

Cell proliferation assay

NB cells were seeded in 96-well plates at a density of 10^4 cells/well in a final volume of 100 μl. Twenty-four hours after seeding, the medium was removed and replaced with fresh medium or with medium containing 0.5 μg/ml of Doxo or 20 μM etoposide in a final volume of 100 μl. The culture was maintained in the 5% CO_2 for 24 h and then 10 μl of WST-8 labeling solution (Cell Counting Kit-8, DOJINDO, Kumamoto, Japan) was added, and the cells were returned to the incubator for 4 h. The absorbance of the formazan product formed was

Table 1 Sequence of primers for PCR experiments

Gene	*Forward primer sequence*	*Reverse primer sequence*	*Accession number*
p53	cagccaagtctgtgacttgcacgtac	ctatgtcgaaaagtgtttctgtcatc	NM_000546
$p21^{Cip1/Waf1}$	gacaccactggagggtgact	ggcgtttggagtggtagaaa	L25610
HDM2	tagtagcattatttatagcagcc	agagaagaaatctatgtgaattgag	Z12020
Noxa	agagctggaagtcgagtgt	gcaccttcacattcctctc	D90070
Bax	ttttgcttcagggtttcatc	cagttgaagttgccgtcaga	BC014175
Bak1	gcctttgcagttggactctc	gggttgggagcaagtgtcta	NM_001188
IFN-α1	caatatctacgatggcctcgc	agagatggctggagccttctg	NM_024013
Caspase-8	gggacaggaatggaacacac	gccatagatgatgcccttgt	AF009620
P-glycoprotein	gaatctggaggaagacatgacc	tccaattttgtcaccaattcc	NM_000927
G3PDH	accacagtccatgccatcac	tccaccaccctgttgctgta	NM_002046

detected at 450 nm in a 96-well spectrophotometric plate reader, as per the manufacturer's protocol.

Morphological analysis of apoptosis and analysis of sub-G_0/G_1 fraction

Cells were observed using a phase-contrast microscope to assess apoptotic morphological changes and treated with 4′,6-diamidino-2-phenylindole (DAPI), a DNA-staining dye, to detect the morphological characteristics of apoptotic nuclei, namely, condensation and fragmentation, after fixation with 3.7% (v/v) formaldehyde/1 × phosphate-buffered saline (PBS). Analysis of sub-G_0/G_1 fraction was performed by using the method described in the previous report (Nakazawa *et al.*, 2003).

Immunofluorescence

Fixation was performed with 3.7% (v/v) formaldehyde/1 × PBS for 30 min and the permeabilization was done with 0.1% (v/v) TritonX-100/1 × PBS for 5 min at room temperature. Cells were then stained for 1 h with the first antibody followed by a 30-min exposure to an appropriate second antibody conjugated with fluorescent dye (Alexa488 or Alexa594). DNA was visualized with DAPI or propidium iodide. Analysis by confocal laser microscopy was performed with an LSM510 system (Carl Zeiss, Oberkochen, Germany).

Cell fractionation and direct western blotting

For the isolation of the heavy membrane faction (Mito) in Figures 4A and B, 2×10^6 cells were subjected to the fractionation procedure described previously (Nakazawa *et al.*, 2003). The resulting supernatant after isolation of Mito was referred to as the cytosol plus light membrane (Cyto) fractions.

For isolation of the nucleus (Nuc) in Figure 2d, 1×10^6 cells were suspended in 0.4 ml of buffer (10 mM HEPES pH 7.9, 10 mM KCl, 1.5 mM $MgCl_2$, 0.5 mM DTT, 0.4 μM PMSF), and incubated on ice for 20 min. After vortexing for 1 min at the maximum setting, cells were centrifuged at 15 000 r.p.m. for 10 s, and then the supernatant was kept as cytosol (Cyto). The pellet was resuspended in 0.1 ml of buffer (20 mM HEPES pH 7.9, 420 mM NaCl, 1.5 mM $MgCl_2$, 0.2 mM EDTA, 25% (v/v) glycerol, 0.5 mM DTT, 0.4 μM PMSF), and incubated on ice for 20 min. Then the cells were centrifuged at 15 000 r.p.m. for 2 min, and then the supernatant was kept as nucleus (Nuc). Direct western blotting was performed according to the previous report (Nakazawa *et al.*, 2003).

Preparation of mRNA and analysis of RNA expression

Total RNA was extracted from NB cells using Isogen (Wako, Tokyo, Japan), and cDNA was synthesized from 1 μg of total RNA templates according to the manufacturer's protocol (RiverTra-Ace-α- RT–PCR kit, TOYOBO, Osaka, Japan). PCR amplification of either p53 or Noxa was performed using previously reported primers (for p53: Paull and Whikehart, 2005; for Noxa: Ohtani *et al.*, 2004). The other primer sequences are listed in Table 1. RT–PCR products (~0.5 kb) were detected by direct ethidium bromide staining after electrophoretic separation on agarose gels. RT–PCR analysis of G3PDH mRNA expression was performed as a positive control for these experiments according to the manufacturer's protocol (RiverTra-Ace -α- RT–PCR kit). Semi-quantitative RT–PCR analysis of tumor samples was performed according to the previous report (Machida *et al.*, 2006). The PCR amplification was performed using the above-mentioned primers for Noxa.

Quantitative real-time PCR analysis

For quantification of Noxa in primary NB samples, cDNA was synthesized with random primers Superscript II reverse transcriptase (GibcoBRL) from 15 μg of primary tumor total RNA. Noxa and GAPDH primers and probes were purchased from Applied Biosystems (Noxa Assay ID: Hs00560402_m1; GAPDH: Pre-Developed TaqMan Assay Reagents Human G3PDH). Quantitative real-time PCR analysis was performed by ABI7700 Prism sequence detector (Applied Biosystems, Foster City, CA, USA), according to the manufacturer's instructions using 1 × TaqMan Universal PCR Master Mix. After denaturing at 95°C for 10 min, PCR amplification was performed by 50 cycles of denaturation at 95°C for 15 s and annealing/extension at 60°C for 1 min. A quantification of *Noxa* mRNA in each sample was performed by comparing with the standard curve, which was generated by reacting the plasmid containing human Noxa (Hijikata *et al.*, 1990). Furthermore, G3PDH mRNA quantification was also performed for a standardization of the initial RNA content of each sample.

Small interference RNA transfection

Noxa small interference RNAs were synthesized according to the previous experiments (Noxa siRNA1, Qin *et al.*, 2004: 5′-TCAGTCTACTGATTTACTGG-3′; Noxa siRNA2, Lee *et al.*, 2005: 5′-AACTTCCGGCAGAAACTTCTG-3′). Control siRNA (Silencer Negative Control #1 siRNA) was purchased from Ambion Inc. (Austin, TX, USA). NB cells were plated at a density of 3×10^5 cells in a 3-cm-diameter dish. Small interference RNA duplexes (10 nM) were transfected with Lipofectamine™ RNAiMAX in Opti-MEM medium according to the manufacturer's protocol. After 24 h, transfected cells were treated with Doxo for another 24 h.

Statistical analysis

The Welch test was used as a statistical method of parametric test to explore possible associations between Noxa expression and other factors, using StatView ver. 4.11 (Abacus Concepts

Inc., Cheltenham, UK). Statistical significance was declared if the P-value was <0.05.

Acknowledgements

We are deeply indebted to Professor Kenichi Koike (Department of Pediatrics, Shinshu University School of Medicine) for his excellent advice. We thank Kumiko Sakurai, Yozo Nakazawa, and Jun Miki for their technical assistance, and Daniel Mrozek, Medical English Service Inc, for editorial assistance. This work was supported by grants from the Japanese Ministry of Education, Science, Sports and Culture, Grant-in-Aid for Scientific Research (C) (contract nos: 15591098 and 17591077).

References

Aleyasin H, Cregan SP, Iyirhiaro G, O'Hare MJ, Callaghan SM, Slack RS *et al.* (2004). Nuclear factor-(kappa)B modulates the p53 response in neurons exposed to DNA damage. *J Neurosci* **24**: 2963–2973.

Bell E, Premkumar R, Carr J, Lu X, Lovat PE, Kees UR *et al.* (2006). The role of MYCN in the failure of MYCN amplified neuroblastoma cell lines to G1 arrest after DNA damage. *Cell Cycle* **5**: 2639–2647.

Danial NN, Korsmeyer SJ. (2004). Cell death: critical control points. *Cell* **116**: 205–219.

Green DR. (2000). Apoptotic pathways: paper wraps stone blunts scissors. *Cell* **102**: 1–4.

Hempel G, Flege S, Wurthwein G, Boos J. (2002). Peak plasma concentrations of doxorubicin in children with acute lymphoblastic leukemia or non-Hodgkin lymphoma. *Cancer Chemother Pharmacol* **49**: 133–141.

Hijikata M, Kato N, Sato T, Kagami Y, Shimotohno K. (1990). Molecular cloning and characterization of a cDNA for a novel phorbol-12-myristate-13-acetate-responsive gene that is highly expressed in an adult T-cell leukemia cell line. *J Virol* **64**: 4632–4639.

Hopkins-Donaldson S, Yan P, Bourloud KB, Muhlethaler A, Bodmer JL, Gross N. (2002). Doxorubicin-induced death in neuroblastoma does not involve death receptors in S-type cells and is caspase-independent in N-type cells. *Oncogene* **21**: 6132–6137.

Hudson CD, Morris PJ, Latchman DS, Budhram-Mahadeo VS. (2005). Brn-3a transcription factor blocks p53-mediated activation of proapoptotic target genes Noxa and Bax *in vitro* and *in vivo* to determine cell fate. *J Biol Chem* **280**: 11851–11948.

Isaacs JS, Saito S, Neckers LM. (2001). Requirement for HDM2 activity in the rapid degradation of p53 in neuroblastoma. *J Biol Chem* **276**: 18497–18506.

Kamijo T, Aoyama T, Miyazaki J, Hashimoto T. (1993). Molecular cloning of the cDNAs for the subunits of rat mitochondrial fatty acid beta-oxidation multienzyme complex. Structural and functional relationships to other mitochondrial and peroxisomal beta-oxidation enzymes. *J Biol Chem* **268**: 26452–26460.

Keshelava N, Zuo JJ, Chen P, Waidyaratne SN, Luna MC, Gomer CJ *et al.* (2001). Loss of p53 function confers high-level multidrug resistance in neuroblastoma cell lines. *Cancer Res* **61**: 6185–6193.

Kiryu-Seo S, Hirayama T, Kato R, Kiyama H. (2005). Noxa is a critical mediator of p53-dependent motor neuron death after nerve injury in adult mouse. *J Neurosci* **25**: 1442–1447.

Komarova EA, Chernov MV, Franks R, Wang K, Armin G, Zelnick CR *et al.* (1997). Transgenic mice with p53-responsive lacZ: p53 activity varies dramatically during normal development and determines radiation and drug sensitivity *in vivo*. *EMBO J* **16**: 1391–1400.

Letai A, Bassik MC, Walensky LD, Sorcinelli MD, Weiler S, Korsmeyer SJ. (2002). Distinct BH3 domains either sensitize or activate mitochondrial apoptosis, serving as prototype cancer therapeutics. *Cancer Cell* **2**: 183–192.

Lee SJ, Kim KM, Namkoong S, Kim CK, Kang YC, Lee H *et al.* (2005). Nitric oxide inhibition of homocysteine-induced human endothelial cell apoptosis by down-regulation of p53-dependent Noxa expression through the formation of S-nitrosohomocysteine. *J Biol Chem* **280**: 5781–5788.

Lowe SW, Bodis S, McClatchey A, Remington L, Ruley HE, Fisher DE *et al.* (1994). p53 status and the efficacy of cancer therapy *in vivo*. *Science* **266**: 807–810.

Machida T, Fujita T, Ooo ML, Ohira M, Isogai E, Mihara M *et al.* (2006). Increased expression of proapoptotic BMCC1, a novel gene with the BNIP2 and Cdc42GAP homology (BCH) domain, is associated with favorable prognosis in human neuroblastomas. *Oncogene* **25**: 1931–1942.

Matthay KK, Perez C, Seeger RC, Brodeur GM, Shimada H, Atkinson JB *et al.* (1998). Successful treatment of stage III neuroblastoma based on prospective biologic staging: a Children's Cancer Group study. *J Clin Oncol* **16**: 1256–1264.

Moll UM, LaQuaglia M, Bénard J, Riou G. (1995). Wild-type p53 protein undergoes cytoplasmic sequestration in undifferentiated neuroblastomas but not in differentiated tumors. *Proc Natl Acad Sci USA* **92**: 4407–4411.

Moll UM, Ostermeyer AG, Haladay R, Winkfield B, Frazier M, Zambetti G. (1996). Cytoplasmic sequestration of wild-type p53 protein impairs the G1 checkpoint after DNA damage. *Mol Cell Biol* **16**: 1126–1137.

Nakazawa Y, Kamijo T, Koike K, Noda T. (2003). ARF tumor suppressor induces mitochondria-dependent apoptosis by modulation of mitochondrial Bcl-2 family proteins. *J Biol Chem* **278**: 27888–27895.

Obexer P, Geiger K, Ambros PF, Meister B, Ausserlechner MJ. (2007). FKHRL1-mediated expression of Noxa and Bim induces apoptosis via the mitochondria in neuroblastoma cells. *Cell Death Diff* **14**: 534–547.

Oda E, Ohki R, Murasawa H, Nemoto J, Shibue T, Yamashita T *et al.* (2003). Noxa, a BH3-only member of the Bcl-2 family and candidate mediator of p53-induced apoptosis. *Science* **17**: 1053–1058.

Oda K, Arakawa H, Tanaka T, Matsuda K, Tanikawa C, Mori T *et al.* (2000). p53AIP1, a potential mediator of p53-dependent apoptosis, and its regulation by Ser-46-phosphorylated p53. *Cell* **102**: 849–862.

Ohtani S, Kagawa S, Tango Y, Umeoka T, Tokunaga N, Tsunemitsu Y *et al.* (2004). Quantitative analysis of p53-targeted gene expression and visualization of p53 transcriptional activity following intratumoral administration of adenoviral p53 *in vivo*. *Mol Cancer Ther* **3**: 93–100.

Oren M. (1999). Regulation of the p53 tumor suppressor protein. *J Biol Chem* **274**: 36031–36034.

Paull AC, Whikehart DR. (2005). Regulation of the p53 tumor suppressor protein. *Mol Vis* **11**: 328–334.

Qin JZ, Stennett L, Bacon P, Bodner B, Hendrix MJ, Seftor RE *et al.* (2004). p53-independent NOXA induction overcomes apoptotic resistance of malignant melanomas. *Mol Cancer Ther* **3**: 895–902.

Shen Y, White E. (2001). p53-dependent apoptosis pathways. *Adv Cancer Res* **82**: 55–84.

Shibue T, Takeda K, Oda E, Tanaka H, Murasawa H, Takaoka A *et al.* (2003). Integral role of Noxa in p53-mediated apoptotic response. *Genes Dev* **17**: 2233–2238.

Shieh SY, Ikeda M, Taya Y, Prives C. (1997). DNA damage-induced phosphorylation of p53 alleviates inhibition by MDM2. *Cell* **91**: 325–334.

Tweddle DA, Malcolm AJ, Bown N, Pearson AD, Lunec J. (2001). Evidence for the development of p53 mutations after cytotoxic therapy in a neuroblastoma cell line. *Cancer Res* **61**: 8–13.

Tweddle DA, Pearson AD, Haber M, Norris MD, Xue C, Flemming C *et al.* (2003). The p53 pathway and its inactivation in neuroblastoma. *Cancer Lett* **197**: 93–98.

Wong HK, Fricker M, Wyttenbach A, Villunger A, Michalak EM, Strasser A *et al.* (2005). Mutually exclusive subsets of BH3-only proteins are activated by the p53 and c-Jun N-terminal kinase/c-Jun signaling pathways during cortical neuron apoptosis induced by arsenite. *Mol Cell Biol* **25**: 8732–8747.

Wei MC, Zong WX, Cheng EH, Lindsten T, Panoutsakopoulou V, Ross AJ *et al.* (2001). Proapoptotic BAX and BAK: a requisite gateway to mitochondrial dysfunction and death. *Science* **292**: 727–730.

Wolff A, Technau A, Ihling C, Technau-Ihling K, Erber R, Bosch FX *et al.* (2001). Evidence that wild-type p53 in neuroblastoma cells is in a conformation refractory to integration into the transcriptional complex. *Oncogene* **20**: 1307–1317.

Yakovlev AG, Di Giovanni S, Wang G, Liu W, Stoica B, Faden AI. (2004). BOK and NOXA are essential mediators of p53-dependent apoptosis. *J Biol Chem* **279**: 28367–28374.

Oncogene (2008) 27, 3700–3709
© 2008 Nature Publishing Group All rights reserved 0950-9232/08 $30.00
www.nature.com/onc

ORIGINAL ARTICLE

A novel HECT-type E3 ubiquitin protein ligase NEDL1 enhances the p53-mediated apoptotic cell death in its catalytic activity-independent manner

Y Li[1,2,3], T Ozaki[1,3], H Kikuchi[1], H Yamamoto[1], M Ohira[1] and A Nakagawara[1]

[1]*Division of Biochemistry, Chiba Cancer Center Research Institute, Nitona, Chuou-Ku, Chiba, Japan and* [2]*Production Technology Development Center, the Furukawa Electric Co., Ltd., 6 Yawata-Kaigandori, Ichihara, Japan*

NEDL1 (NEDD4-like ubiquitin protein ligase-1) is a newly identified HECT-type E3 ubiquitin protein ligase highly expressed in favorable neuroblastomas as compared with unfavorable ones. In this study, we found that NEDL1 cooperates with p53 to induce apoptosis. During cisplatin (CDDP)-mediated apoptosis in neuroblastoma SH-SY5Y cells, p53 was induced to accumulate in association with an increase in expression levels of NEDL1. Enforced expression of NEDL1 resulted in a decrease in number of G418-resistant colonies in SH-SY5Y and U2OS cells bearing wild-type *p53*, whereas NEDL1 had undetectable effect on *p53*-deficient H1299 and SAOS-2 cells. Similarly, enforced expression of NEDL1 increased number of U2OS cells with sub-G1 DNA content. Co-immunoprecipitation and *in vitro* binding assays revealed that NEDL1 binds to the COOH-terminal region of p53. Luciferase reporter assay showed that NEDL1 has an ability to enhance the transcriptional activity of p53. Small interfering RNA-mediated knockdown of the endogenous NEDL1 conferred the resistance of U2OS cells to adriamycin. It is noteworthy that NEDL1 enhanced pro-apoptotic activity of p53 in its catalytic activity-independent manner. Taken together, our present findings suggest that functional interaction of NEDL1 with p53 might contribute to the induction of apoptosis in cancerous cells bearing wild-type *p53*.

Oncogene (2008) **27,** 3700–3709; doi:10.1038/sj.onc.1211032; published online 28 January 2008

Keywords: apoptosis; cisplatin; DNA damage; HECT-type E3 ubiquitin ligase; NEDL1; p53

Introduction

NEDL1 (NEDD4-like ubiquitin protein ligase-1), which has been identified as a novel gene expressed significantly at high levels in favorable neuroblastomas relative to unfavorable ones, encodes HECT-type E3 ubiquitin ligase and is detected specifically in human neuronal tissues (Miyazaki *et al.*, 2004), suggesting that NEDL1 might be involved in the regulation of the spontaneous regression of favorable neuroblastomas caused by apoptosis and/or neuronal differentiation. According to our previous findings, NEDL1 ubiquitinated mutant forms of SOD1 (superoxide dismutase-1) as well as Dvl-1 (Dishevelled-1), thereby promoting their proteasome-dependent degradation (Miyazaki *et al.*, 2004). SOD1 mutations have been detected in a certain subset of patients with familial amyotrophic lateral sclerosis, which is one of the fatal neurological diseases in human, and mutant SOD1 aggregates to form insoluble macromolecular protein complexes in motor neurons and astrocytes (Cluskey and Ramsden, 2001), suggesting that the accumulation of misfolded proteins generates cellular stresses to induce neuronal cell death. However, the precise molecular mechanisms behind the possible contribution of NEDL1 to apoptosis in motor neurons remain elusive.

As described previously (Gonzalez de Aguilar *et al.*, 2000), pro-apoptotic Bax, which is one of the direct targets of tumor suppressor p53 (Roos and Kaina, 2006), accumulated in central nervous system regions in patients with amyotrophic lateral sclerosis. In support of this notion, p53 was induced in central nervous system regions in patients and also in model mice with amyotrophic lateral sclerosis (Martin, 2000), indicating that p53-mediated pro-apoptotic pathway plays an important role in the regulation of neuronal apoptosis. p53 is a nuclear transcription factor that induces cell cycle arrest and/or apoptosis. Under normal conditions, p53 is kept at extremely low level. The expression of p53 is regulated largely at protein level. For example, E3 ubiquitin ligase MDM2 inhibits transactivation activity of p53 and also promotes its ubiquitination-mediated proteasomal degradation (Vousden and Lu, 2002). In response to genotoxic stresses, p53 is induced to be converted from the latent form to the active one through the post-translational modifications such as phosphorylation and acetylation, and thereby transactivating its direct target genes implicated in cell cycle arrest and/or apoptosis including $p21^{WAF1}$, *MDM2*, *Bax*, *Puma*, *Noxa* and *p53AIP1* (Vousden and Lu, 2002). Accumulating evidence strongly suggests that its transactivation

Correspondence: Dr A Nakagawara, Division of Biochemistry, Chiba Cancer Center Research Institute, 666-2 Nitona, Chuou-Ku, Chiba 260-8717, Japan.
E-mail: akiranak@chiba-cc.jp
[3]These authors contributed equally to this work.
Received 16 May 2007; revised 26 November 2007; accepted 10 December 2007; published online 28 January 2008

activity is tightly linked to its pro-apoptotic function (Pietenpol *et al*., 1994). Consistent with this notion, majority of loss-of-function mutations of p53 in a variety of primary human tumors is detected within its DNA-binding domain (Hollstein *et al*., 1991; Levine *et al*., 1994) and *p53*-deficient mice developed spontaneous tumors (Donehower *et al*., 1992).

In the present study, we found that NEDL1 binds to the COOH-terminal region of p53 and enhances its transcriptional activity as well as pro-apoptotic function in its catalytic activity-independent manner. Our present findings suggest that NEDL1 plays a pivotal role in the induction of apoptosis in cancerous cells bearing wild-type *p53* through the interaction with p53 and also might provide a novel insight into understanding neuronal dysfunction.

Results

NEDL1 has a pro-apoptotic function

As described previously (Miyazaki *et al*., 2004), we cloned a novel gene termed *NEDL1* from the oligo-capping cDNA libraries prepared from a mixture of fresh primary neuroblastoma tissues that underwent spontaneous regression (Nakagawara and Ohira, 2004). *NEDL1* was highly expressed in favorable neuroblastomas as compared with unfavorable ones and significantly associated with better prognosis in neuroblastoma (Supplementary Figure S1). To examine the expression levels of NEDL1 in response to DNA damage, human neuroblastoma SH-SY5Y cells bearing wild-type *p53* were exposed to 20 μM of cisplatin (CDDP). At the indicated time periods, cells were subjected to terminal deoxynucleotidyl transferase-mediated dUTP-biotin nick end labeling (TUNEL) staining. As shown in Figure 1a, SH-SY5Y cells underwent apoptosis in a time-dependent manner. We then analysed the expression patterns of NEDL1 and p53 in response to CDDP. As shown in Figures 1b and c, p53 was induced to accumulate at protein level but not at mRNA level and CDDP treatment promoted phosphorylation of p53 at Ser-15 in association with a significant upregulation of various p53 target genes such as $p21^{WAF1}$, *Bax* and *Noxa*. It is noteworthy that NEDL1 increased at both mRNA and protein levels in SH-SY5Y cells exposed to CDDP in a time-dependent manner. *NEDL1* was also upregulated in *p53*-deficient human lung carcinoma H1299 cells in response to CDDP (Figure 1d), indicating that *NEDL1* might not be a direct target of p53. Since a correlation between expression levels of NEDL1 and p53 was observed in SH-SY5Y cells treated with CDDP, it is likely that there could exist a functional interaction between them during DNA damage-mediated apoptotic response.

To confirm this notion, we performed colony formation assay. *p53*-proficient SH-SY5Y, human osteosarcoma U2OS, *p53*-deficient human lung carcinoma H1299 and human osteosarcoma SAOS-2 cells were transfected

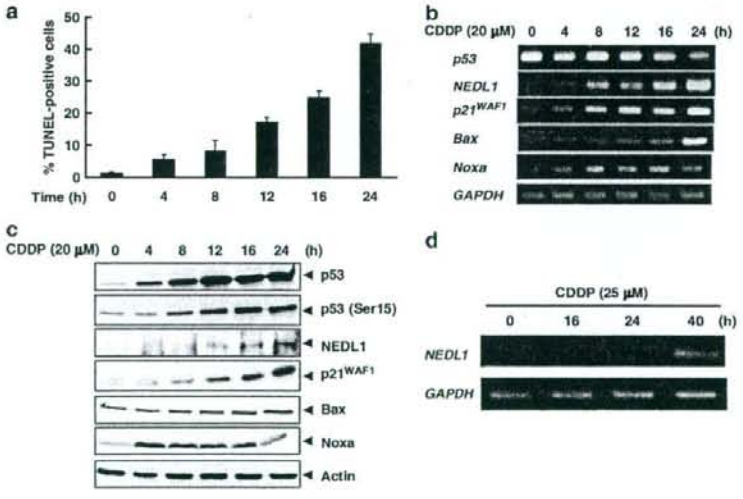

Figure 1 NEDL1 is induced to accumulate in response to CDDP. (**a**) CDDP-mediated apoptosis. SH-SY5Y cells were treated with CDDP (20 μM). Cells were then stained with an *in situ* cell death detection kit followed by mounting with 4′,6-diamidino-2-phenylindole-containing mounting medium. The number of TUNEL-positive cells was scored. Results were expressed as means ± s.d. of three independent experiments. (**b** and **c**) Expressions of NEDL1 and p53 in response to CDDP. Total RNA and cell lysates were prepared from SH-SY5Y cells exposed to CDDP for the indicated time periods and subjected to RT PCR (**b**) and immunoblotting (**c**), respectively. (**d**) *NEDL1* is induced in *p53*-deficient H1299 cells exposed to CDDP. H1299 cells were treated with 25 μM of CDDP. At the indicated time points, total RNA was prepared and analysed for the expression levels of *NEDL1* by RT PCR. *GAPDH* was used as an internal control. CDDP, cisplatin; GAPDH, glyceraldehyde-3-phosphate dehydrogenase; NEDL1, NEDD4-like ubiquitin protein ligase-1; RT PCR, reverse transcription PCR; TUNEL, terminal deoxynucleotidyl transferase-mediated dUTP-biotin nick end labeling.

with empty plasmid or with expression plasmid for NEDL1. Following 2 weeks of selection with G418, drug-resistant colonies were stained and photographed. As shown in Figures 2a and b, enforced expression of NEDL1 caused a significant decrease in the number of drug-resistant colonies in *p53*-proficient SH-SY5Y and U2OS cells relative to control cells, whereas NEDL1 had undetectable effects on *p53*-deficient H1299 and SAOS-2 cells, indicating that NEDL1 induces cell cycle arrest and/or apoptosis in cells carrying wild-type *p53*.

To address whether NEDL1 could cooperate with p53 to induce cell cycle arrest and/or apoptosis, we checked NEDL1-mediated proteolytic cleavage of caspase-3. For this purpose, expression plasmid for NEDL1 was introduced into the indicated cells. As shown in Figure 3a, NEDL1-mediated proteolytic cleavage of caspase-3 was detectable in SH-SY5Y and U2OS cells, but not in H1299 and SAOS-2 cells. Furthermore, enforced expression of NEDL1 resulted in an increase in the number of U2OS cells with sub-G1 DNA content (Figure 3b), whereas NEDL1 had negligible effects on SAOS-2 cells (Figure 3c). Since U2OS cells expressed wild-type p53, these findings suggest that NEDL1 induces apoptosis in a p53-dependent manner.

Interaction between NEDL1 and p53

To determine whether NEDL1 could interact with p53, COS7 cells were transfected with NEDL1 expression plasmid. As shown in Figure 4a, the anti-NEDL1 immunoprecipitates contained endogenous p53. To further confirm this issue, cell lysates prepared from U2OS cells exposed to CDDP were immunoprecipitated with normal rabbit serum or with anti-NEDL1 antibody and analysed by immunoblotting with anti-p53 antibody. As shown in Figure 4b, the anti-NEDL1 immunoprecipitates contained endogenous p53, suggesting that NEDL1 associates with endogenous p53 in cells. In contrast to wild-type p53, mutant form of p53 was not co-immunoprecipitated with NEDL1 (Figure 4c). To identify the region(s) of p53 responsible for the interaction with NEDL1, we performed *in vitro* pull-down assay using the indicated radio-labeled p53 deletion mutants. As clearly shown in Figure 4d, full-length p53, p53(1–353) and p53(102–393) were co-immunoprecipitated with NEDL1, whereas remaining p53 deletion mutants including p53(1–292) and p53(1–102) were not. Under our experimental conditions, other p53 family members such as p73 and p63 failed to be co-immunoprecipitated with NEDL1 (data not shown). These results suggest that NEDL1 specifically interacts with COOH-terminal region of p53 (amino-acid residues 293–353) and might modulate p53 function.

NEDL1 enhances the transcriptional activity of p53

Next, we sought to examine a possible effect of NEDL1 on the transcriptional activity of p53. H1299 cells were co-transfected with a constant amount of p53 expression plasmid, together with p53-responsive $p21^{WAF1}$ or *Bax* luciferase reporter construct in the presence or absence of increasing amounts of NEDL1 expression plasmid. As shown in Figures 5a and b, enforced expression of NEDL1 enhanced p53-mediated transactivation toward $p21^{WAF1}$ and *Bax* promoters in a dose-dependent manner. Similarly, luciferase activities driven by $p21^{WAF1}$ promoter were increased by NEDL1 in U2OS cells (Figure 5c). In support of these results, reverse transcription–polymerase chain reaction (RT–PCR) analysis showed that enforced expression of NEDL1 led to a significant increase in expression levels of endogenous $p21^{WAF1}$ and *Noxa* induced by exogenously

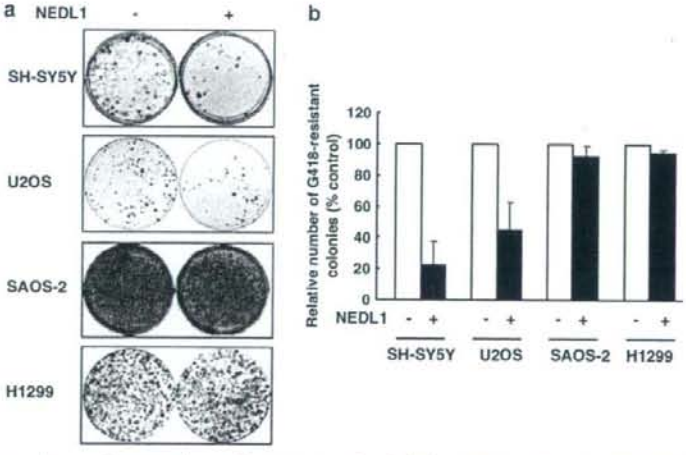

Figure 2 NEDL1 exerts its growth-suppressive and/or pro-apoptotic activity in cancerous cells bearing wild-type *p53*. (**a**) SH-SY5Y cells and U2OS cells harboring wild-type *p53* as well as *p53*-deficient H1299 cells and SAOS-2 cells were transfected with 2.0 μg of empty plasmid (pcDNA3) or with 2.0 μg of expression plasmid for NEDL1. Forty-eight hours after transfection, cells were transferred to fresh medium containing G418 (400 μg ml^{-1}). Two weeks after selection, drug-resistant colonies were stained with Giemsa's solution and photographed. (**b**) Average number of drug-resistant colonies in each transfection relative to pcDNA3 empty plasmid control (set at 100%). Results were expressed as means ± s.d. of three independent experiments. NEDL1, NEDD4-like ubiquitin protein ligase-1.

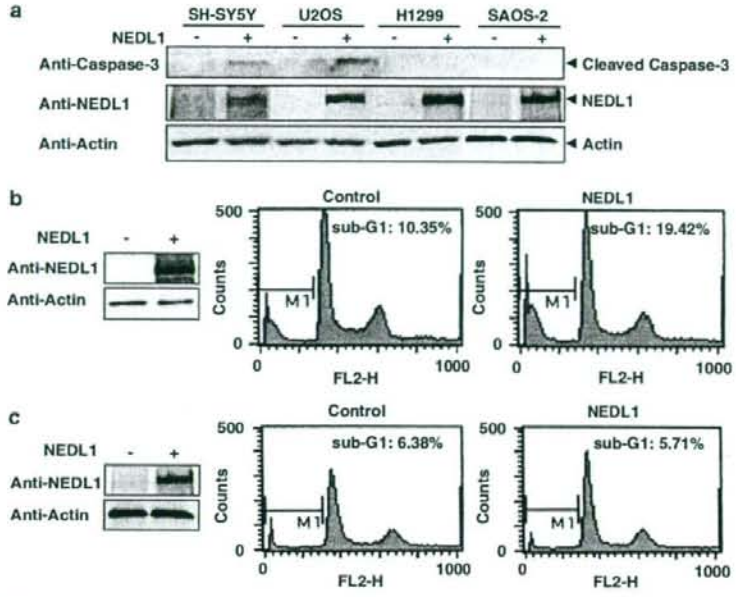

Figure 3 NEDL1 has a pro-apoptotic activity in cells bearing wild-type *p53*. (**a**) Cleavage of caspase-3. Expression plasmid encoding NEDL1 or empty plasmid was transfected into the indicated cells. Forty-eight hours after transfection, cell lysates were prepared and processed for immunoblotting with the indicated antibodies. (**b** and **c**) FACS analysis. U2OS (**b**) and SAOS-2 (**c**) cells were transfected with empty plasmid or with expression plasmid for NEDL1. Forty-eight hours after transfection, expression levels of NEDL1 were examined by immunoblotting (left panels) and number of cells with sub-G1 DNA content was analysed by FACS (right panels). NEDL1, NEDD4-like ubiquitin protein ligase-1.

expressed p53 (Figure 5d). Furthermore, chromatin immunoprecipitation (ChIP) assay demonstrated that NEDL1 has an ability to increase the amounts of exogenous and endogenous p53 recruited onto $p21^{WAF1}$ promoter region, whereas NEDL1 alone is not recruited onto $p21^{WAF1}$ promoter region (Figure 5e), indicating that NEDL1 might cooperate with p53 to directly induce the transcription of p53 target genes.

NEDL1 enhanced the pro-apoptotic activity of p53 independent of its ubiquitin ligase activity

Since NEDL1 has an intrinsic E3 ubiquitin ligase activity (Miyazaki *et al.*, 2004), these results prompted us to examine whether NEDL1 could ubiquitinate p53. In spite of our extensive efforts, we could not detect NEDL1-mediated ubiquitination of p53 (Supplementary Figure S2). Under our experimental conditions, NEDL1 efficiently ubiquitinated Dvl-1 as described previously (Miyazaki *et al.*, 2004), whereas HECT(−) mutant failed to ubiquitinate Dvl-1. To extend these observations, we examined a possible effect of NEDL1 catalytic activity on pro-apoptotic function of p53. H1299 cells were co-transfected with a constant amount of expression plasmid for p53 together with or without increasing amounts of wild-type NEDL1 or mutant form of NEDL1 lacking HECT domain termed HECT(−) (Figure 6a). Following 2 weeks of selection with G418 (400 μg ml^{-1}), drug-resistant colonies were stained with Giemsa's solution. Enforced expression of p53 decreased the number of drug-resistant colonies as compared with that in control cells (Figure 6b). As expected, coexpression of p53 plus wild-type NEDL1 or HECT(−) mutant led to a dramatic decrease in the number of drug-resistant colonies in a dose-dependent manner relative to that in cells expressing p53 alone. *In vitro* pull-down assay demonstrated that HECT(−) mutant, but not CW linker, retains an ability to interact with p53 (Figure 6c). In addition, CW linker had negligible effects on the transcriptional activity of p53 (Supplementary Figure S3). Thus, it is likely that NEDL1 enhances the transcriptional as well as pro-apoptotic function of p53 in its catalytic activity-independent manner.

siRNA-mediated knockdown of endogenous NEDL1 confers resistance of U2OS cells to adriamycin

To address the physiological role of endogenous NEDL1 in response to DNA damage, we designed small interfering RNAs (siRNAs) against NEDL1 termed nos. 1, 2, 3 and 4. U2OS cells were transfected with the indicated siRNAs. As shown in Figure 7a, nos. 2, 3 and 4 siRNAs successfully knocked down the endogenous *NEDL1*. We then used nos. 2 and 4 siRNAs for further experiments.

To examine the possible effect of siRNA targeting NEDL1 on the sensitivity to adriamycin (ADR), U2OS cells were transfected with control siRNA, no. 2 or 4 siRNA. Twenty-four hours after transfection, cells were

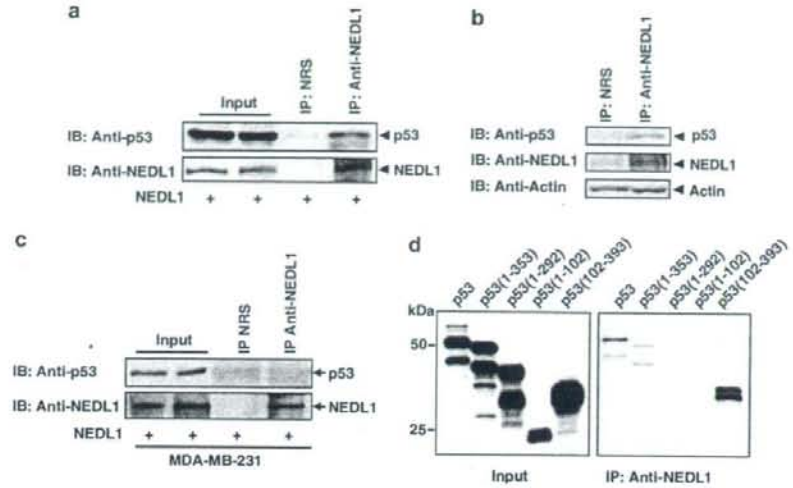

Figure 4 Interaction between NEDL1 and p53. (**a**) Immunoprecipitation. COS7 cells were transfected with NEDL1 expression plasmid. Forty-eight hours after transfection, cell lysates were prepared and immunoprecipitated with NRS or with polyclonal anti-NEDL1 antibody. Immunoprecipitates were analysed by immunoblotting with the indicated antibodies. Ten percentage of inputs were also loaded (input). (**b**) Endogenous interaction between NEDL1 and p53. U2OS cells were exposed to CDDP (20 μM). Twenty-four hours after CDDP treatment, cell lysates prepared from U2OS cells were immunoprecipitated with NRS or with anti-NEDL1 antibody and analysed by immunoblotting with anti-p53 antibody (top panel). The anti-NEDL1 immunoprecipitates contained endogenous NEDL1 (middle panel). To show that equal amounts of cell lysates are used for immunoprecipitation, expression of actin was examined (bottom panel). (**c**) Mutant form of p53 does not bind to NEDL1. Human breast cancer MDA-MB-231 cells, in which Arg at 280 is substituted with Lys, were transfected with expression plasmid for NEDL1. Forty-eight hours after transfection, cell lysates were immunoprecipitated with polyclonal anti-NEDL1 antibody or with NRS and the immunoprecipitates were analysed by immunoblotting with the indicated antibodies. Ten percentage of inputs are also shown (input). (**d**) The indicated p53 derivatives were labeled with [^{35}S]methionine *in vitro* and incubated with cell lysates prepared from COS7 cells transfected with expression plasmid for NEDL1. The reaction mixtures were immunoprecipitated with anti-NEDL1 antibody and the immunoprecipitates were analysed by sodium dodecyl sulfate polyacrylamide gel electrophoresis. The gels were then dried and subjected to autoradiography. CDDP, cisplatin; NEDL1, NEDD4-like ubiquitin protein ligase-1; NRS, normal rabbit serum.

exposed to the indicated concentrations of ADR for 24 h followed by fluorescence-activated cell sorter (FACS) analysis. As shown in Figure 7b, U2OS cells transfected with control siRNA underwent apoptosis in a dose-dependent manner. In contrast, the number of cells with sub-G1 DNA content in response to ADR was significantly decreased in U2OS cells transfected with siRNAs against NEDL1 relative to cells expressing control siRNA. Similarly, siRNA-mediated knockdown of endogenous NEDL1 led to a remarkable decrease in the number of apoptotic cells caused by ADR in a time-dependent manner (Figure 7c).

Next, we determined whether siRNA-mediated knockdown of endogenous NEDL1 could inhibit the transcriptional activation of p53 target genes in response to ADR. U2OS cells were transfected with the indicated siRNAs. Twenty-four hours after transfection, cells were treated with ADR for 24 h. As shown in Figure 8a, ADR treatment induced the accumulation of p53 and phosphorylated form of p53 at Ser-15. However, siRNA-mediated knockdown of endogenous NEDL1 had negligible effects on amounts of p53 and phosphorylated form of p53 at Ser-15 in response to ADR, suggesting that their interaction does not affect the stability of p53 in response to DNA damage. It is noteworthy that expression levels of Noxa increased in cells exposed to ADR, whereas ADR-mediated upregulation of Noxa was markedly inhibited in NEDL1-knocked down U2OS cells. RT–PCR analysis also demonstrated that siRNA-mediated knockdown of endogenous NEDL1 reduces the transcription of p53 target genes such as *Noxa* and *Puma* induced by ADR (Figure 8b). ADR treatment had undetectable effects on *p53* (data not shown). Intriguingly, NEDL1 increased the acetylation levels of p73 (Figure 8c). Taken together, our present results suggest that NEDL1 has an ability to enhance the transcriptional and pro-apoptotic activities of p53 through the interaction without affecting its stability.

Discussion

In the present study, we have found that a novel HECT-type E3 ubiquitin ligase NEDL1 has the ability to cooperate with p53 to induce apoptosis.

During CDDP-mediated apoptosis in SH-SY5Y cells carrying wild-type *p53*, expression levels of NEDL1 correlated with those of p53. Expression levels of *NEDL1* were higher in favorable neuroblastoma than those in unfavorable neuroblastoma. Favorable neuroblastoma undergoes spontaneous regression through

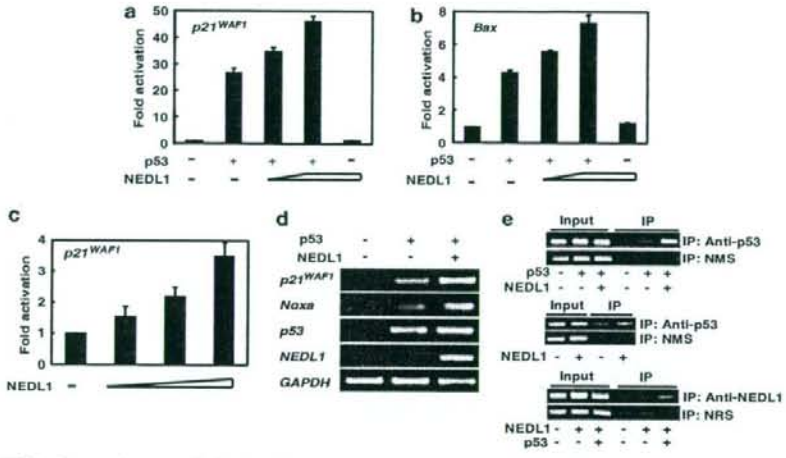

Figure 5 NEDL1 enhances the transcriptional activity of p53. (**a** and **b**) Luciferase reporter assays. H1299 cells were co-transfected with 25 ng of expression plasmid for p53, 100 ng of luciferase reporter construct containing p53-responsive element derived from *p21*^{WAF1} (**a**) or *Bax* (**b**) promoter and 10 ng of *Renilla* luciferase plasmid (pRL-TK) together with or without increasing amounts of expression plasmid for NEDL1 (475 and 875 ng). Total amount of plasmid DNA per transfection was kept constant (1 μg) with pcDNA3. Forty-eight hours after transfection, cell lysates were prepared and their luciferase activity was measured. Data were normalized to the *Renilla* luciferase activity. (**c**) Luciferase reporter assays. U2OS cells were co-transfected with 100 ng of luciferase reporter construct containing p53-responsive element derived from *p21*^{WAF1} promoter and 10 ng of pRL-TK together with or without increasing amounts of expression plasmid for NEDL1 (400, 800 and 1000 ng). Forty-eight hours after transfection, cell lysates were prepared and their luciferase activity was measured as described above. (**d**) RT PCR analysis. H1299 cells were co-transfected with a constant amount of p53 expression plasmid (0.1 μg) along with or without NEDL1 expression plasmid (1.9 μg). Forty-eight hours after transfection, total RNA was isolated and subjected to RT PCR analysis. *GAPDH* was used as an internal control. (**e**) ChIP assay. The increased binding of p53 to the promoter region of *p21*^{WAF1} caused by NEDL1 was demonstrated by ChIP assay with chromatin isolated from H1299 cells transfected with the indicated combinations of expression plasmids. As a control, PCR was performed on chromatin fragments isolated both before (input) and after (IP) immunoprecipitation with monoclonal anti-p53 antibody or with normal mouse serum (NMS) (upper panels). Middle panels show the increased binding of endogenous p53 to *p21*^{WAF1} promoter in the presence of NEDL1. Crosslinked chromatin isolated from U2OS cells transfected with or without NEDL1 expression plasmid exposed to adriamycin was subjected to ChIP assay. Lower panels show ChIP assay using crosslinked chromatin prepared from H1299 cells transfected with the indicated combinations of expression plasmids. Crosslinked chromatin was immunoprecipitated with polyclonal anti-NEDL1 or with NRS and subjected to PCR. CDDP, cisplatin; ChIP, chromatin immunoprecipitation; GAPDH, glyceraldehyde-3-phosphate dehydrogenase; NEDL1, NEDD4-like ubiquitin protein ligase-1; NRS, normal rabbit serum; RT PCR, reverse transcriptase PCR.

apoptosis and/or neuronal differentiation (Kitanaka *et al*., 2002). In contrast to other human tumors, *p53* is rarely mutated in neuroblastoma (Moll *et al*., 1995). Thus, it is likely that functional interaction between NEDL1 and p53 might contribute to induction of spontaneous regression caused by apoptosis of favorable neuroblastoma bearing wild-type *p53*. In support of this notion, enforced expression of NEDL1 reduced the number of drug-resistant colonies in cells with wild-type *p53* but not in *p53*-deficient cells. Furthermore, siRNA-mediated knockdown of endogenous NEDL1 inhibited DNA damage-induced apoptosis in cells bearing wild-type *p53*. Our present results demonstrated that NEDL1 binds to COOH-terminal region of p53 and enhances its transcriptional activation. In addition, NEDL1 increased the amounts of p53 recruited onto *p21*^{WAF1} promoter region. As described previously (Hupp and Lane, 1994), COOH-terminal region of p53 masked its DNA-binding domain to inhibit its transcriptional potential. Chemical modifications at COOH-terminal portion of p53, such as acetylation and glycosylation, lead to an increase in the transcriptional activity of p53 (Shaw *et al*., 1996; Thomas and Chiang, 2005; Di Lello *et al*., 2006). In accordance with this notion, enforced expression of NEDL1 resulted in an increase in acetylation levels of p53. Thus, it is possible that the interaction between NEDL1 and p53 might help to expose DNA-binding domain of p53 through the induction of acetylation of p53, and thereby enhance its transcriptional activity. However, the precise molecular mechanisms behind NEDL1-mediated induction of acetylation of p53 remained unclear. Further studies should be necessary to address this issue.

Although we found that NEDL1 has an intrinsic E3 ubiquitin ligase activity (Miyazaki *et al*., 2004), our extensive efforts failed to detect NEDL1-mediated ubiquitination of p53 and enforced expression of NEDL1 had undetectable effects on the stability of endogenous p53 (data not shown). Under our experimental conditions, MDM2 promoted ubiquitination-mediated degradation of p53 (data not shown). NEDL1 and mutant form of NEDL1 lacking its catalytic HECT domain had an ability to decrease the number of drug-resistant colonies in H1299 cells co-transfected with p53 expression plasmid. Like wild-type NEDL1, this NEDL1 mutant retained an ability to interact with

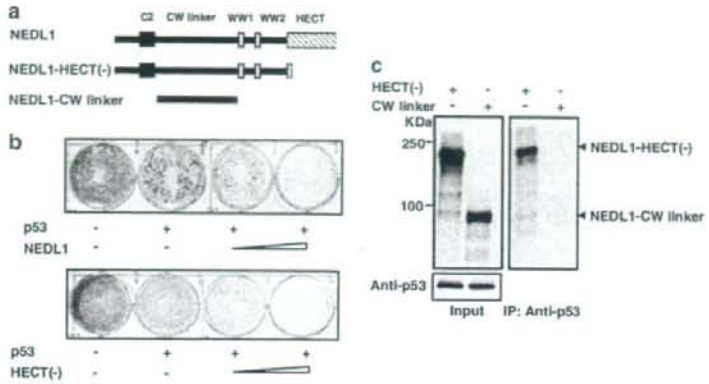

Figure 6 NEDL1 increases pro-apoptotic activity of p53 in its catalytic activity-independent manner. (**a**) Schematic diagram of wild-type NEDL1 and its deletion mutants. (**b**) Colony formation assay. H1299 cells were co-transfected with constant amount of p53 expression plasmid (25 ng) together with or without increasing amounts of expression plasmid for NEDL1 (475 and 975 ng) (upper panel) or NEDL1 lacking HECT domain (475 and 975 ng) (lower panel). Forty-eight hours after transfection, cells were grown in the fresh medium containing G418 (400 μg ml^{-1}). Following 2 weeks selection, drug-resistant colonies were stained with Giemsa's solution. (**c**) *In vitro* pull-down assay. Cell lysates prepared from COS7 cells were incubated with the indicated radio-labeled NEDL1 mutants and then immunoprecipitated with anti-p53 antibody. The immunoprecipitates were subjected to autoradiography (right panel). Left panel shows the autoradiography of the radio-labeled NEDL1 deletion mutants generated by *in vitro* transcription/translation system. NEDL1, NEDD4-like ubiquitin protein ligase-1.

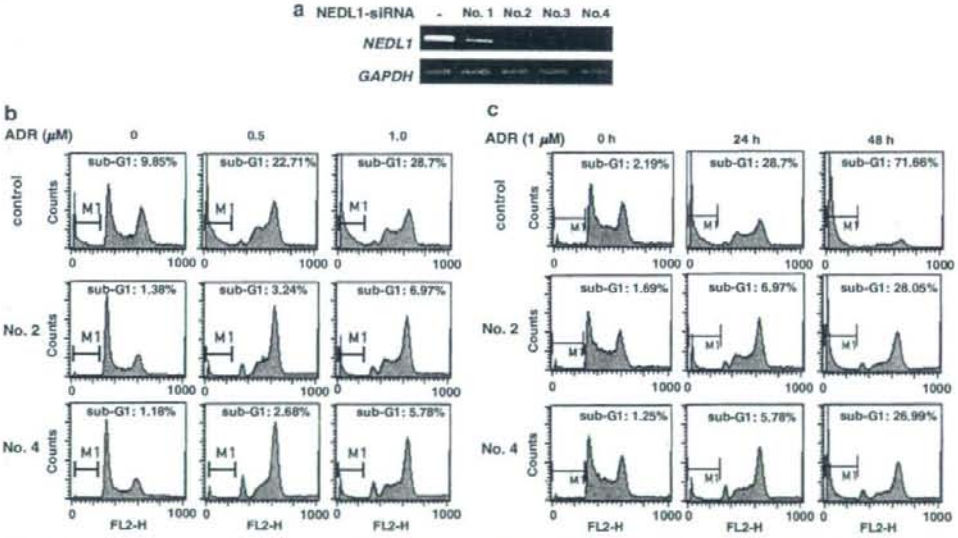

Figure 7 siRNA-mediated knockdown of endogenous NEDL1 confers resistance of U2OS cells to ADR. (**a**) siRNA-mediated knockdown of endogenous NEDL1. U2OS cells were transfected with control siRNA (−), siRNA against NEDL1 termed no. 1, 2, 3 or 4 siRNA. Forty-eight hours after transfection, total RNA was prepared and subjected to reverse transcriptase PCR. *GAPDH* was used as an internal control. (**b**) U2OS cells were transfected with control siRNA, no. 2 or 4 siRNA. Twenty-four hours after transfection, cells were exposed to the indicated concentrations of ADR for 24 h and then cell cycle distributions of cells were analysed by FACS. (**c**) U2OS cells were transfected with control siRNA, no. 2 or 4 siRNA. Twenty-four hours after transfection, cells were treated with ADR (1 μM). At the indicated time periods, cell cycle distributions of cells were analysed by FACS. ADR, adriamycin; GAPDH, glyceraldehyde-3-phosphate dehydrogenase; NEDL1, NEDD4-like ubiquitin protein ligase-1; siRNA, small interfering RNA.

p53 but not ubiquitinate p53. Thus, it is conceivable that the interaction of NEDL1 with p53 suppresses the inhibitory effect of COOH-terminal region of p53 on its function in its catalytic activity-independent manner.

In contrast to p53, NEDL1 did not interact with other p53 family members such as p73 and p63 (data not shown). Intriguingly, we reported that NEDL2, a close relative to NEDL1, binds to PY motif of p73 and

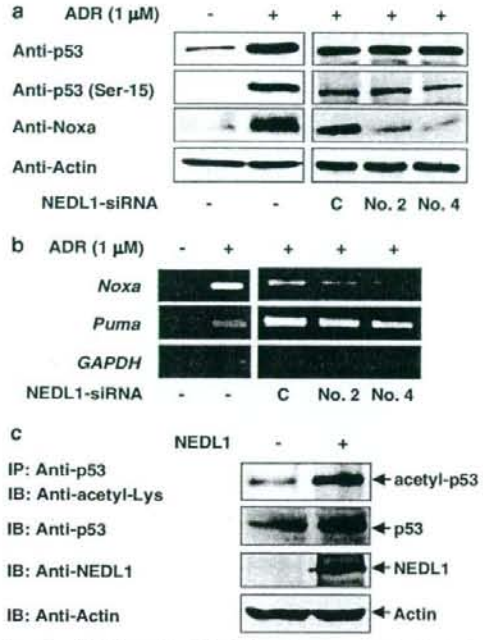

Figure 8 siRNA-mediated depletion of endogenous NEDL1 does not affect the stability of p53 but inhibits ADR-mediated upregulation of p53 target genes. (**a**) U2OS cells were treated with or without ADR (1 μM). Twenty-four hours after the treatment, cell lysates were prepared and subjected to immunoblotting with the indicated antibodies (left panels). U2OS cells were transfected with control siRNA (C), no. 2 or 4 siRNA. Twenty-four hours after transfection, cells were treated with ADR. At the indicated time periods, cell lysates were prepared and processed for immunoblotting with the indicated antibodies (right panels). (**b**) RT PCR analysis. U2OS cells were treated as in (**a**), and total RNA was prepared and subjected to RT PCR. (**c**) NEDL1-mediated increase in acetylation levels of p53. U2OS cells were transfected with empty plasmid or with expression plasmid for NEDL1. Forty-eight hours after transfection, cell lysates were immunoprecipitated with monoclonal anti-p53 antibody. The immunoprecipitates were analysed by immunoblotting with polyclonal anti-acetyl-Lys antibody (New England Biolabs, Ipswich, MA, USA). Expression levels of total p53, NEDL1 and actin were also examined. ADR, adriamycin; GAPDH, glyceraldehyde-3-phosphate dehydrogenase; NEDL1, NEDD4-like ubiquitin protein ligase-1; RT PCR, reverse transcriptase PCR; siRNA, small interfering RNA.

promotes ubiquitination of p73 (Miyazaki *et al.*, 2003). According to our previous results, NEDL2-mediated ubiquitination of p73 increased the stability and activity of p73, raising a possibility that ubiquitination does not always act as a degradation signal. Consistent with our results, ubiquitination was required for the transcriptional activity of c-myc (Adhikary *et al.*, 2005). It is noteworthy that NEDL2 did not interact with p53 that lacks PY motif and had negligible effects on p53 (Miyazaki *et al.*, 2003), indicating that NEDL1 family members have a differential effect on p53 family members. In this regard, it is of interest to examine whether there could exist a functional interaction between NEDL1 family members and p63 that contains PY motif.

Several lines of evidence suggest that pro-apoptotic p53 signaling pathway is involved in motor neuron death associated with amyotrophic lateral sclerosis through an upregulation of pro-apoptotic Bax (Ekegren *et al.*, 1999; Gonzalez de Aguilar *et al.*, 2000; Martin and Liu, 2002). Recently, it has been shown that Noxa is one of the critical mediators of p53-dependent motor neuron death (Kiryo-Seo *et al.*, 2005). These observations suggest that pro-apoptotic p53 signaling pathway plays a causable role in the regulation of neuronal cell death. Thus, it is likely that NEDL1 is involved in the regulation of this cellular process through the interaction with p53.

As described previously (Miyazaki *et al.*, 2004), we found that Dvl-1, a highly conserved cytoplasmic phosphoprotein implicated in Wnt signaling pathway, is one of the physiological targets of NEDL1. On the basis of our previous results, NEDL1 ubiquitinated Dvl-1 and induced its degradation in a proteasome-dependent manner. It has been well documented that Dvl-1 increases the stability of β-catenin through the inhibition of the catalytic activity of glycogen synthase kinase-3β (GSK-3β) (Kishida *et al.*, 2001; Lee *et al.*, 2001; Hino *et al.*, 2003). In addition, GSK-3β facilitated staurosporine-mediated apoptosis in SH-SY5Y cells (Bijur *et al.*, 2000) and also contributed to neuronal apoptosis induced by trophic withdrawal (Hetman *et al.*, 2000). Consistent with these results, specific inhibition of GSK-3β activity by a small chemical compound protected primary neuron from apoptosis (Cross *et al.*, 2001). These results suggest that GSK-3β activity is closely involved in the induction of neuronal cell death. It is worth noting that GSK-3β interacts with p53 in response to DNA damage and enhances pro-apoptotic function of p53 (Watcharasit *et al.*, 2002). Taken together, there exists a functional interaction among NEDL1, Dvl-1, p53 and GSK-3β, which might play a pivotal role at least in part in the regulation of apoptosis in response to DNA damage. Further studies should be necessary to address this issue.

Materials and methods

Cell culture and transfection

COS7, U2OS and SAOS-2 cells were maintained in Dulbecco's modified Eagle's medium supplemented with 10% of heat-inactivated fetal bovine serum (Invitrogen, Carlsbad, CA, USA), penicillin (100 IU ml^{-1}) and streptomycin (100 μg ml^{-1}). *p53*-deficient H1299 and SH-SY5Y cells were grown in RPMI-1640 medium supplemented with 10% heat-inactivated fetal bovine serum and antibiotic mixture. Cells were cultured at 37 °C in a water-saturated atmosphere of 95% air and 5% CO_2. Transient transfection was performed using LipofectAMINE 2000 transfection reagent (Invitrogen) according to the manufacturer's instructions.

Immunoblotting and immunoprecipitation

For immunoblotting, cells were lysed in a lysis buffer containing 25 mM Tris-Cl pH 7.5, 137 mM NaCl, 2.7 mM

KCl, 1% Triton X-100 and protease inhibitor cocktail. Equal amounts of cell lysates were separated by sodium dodecyl sulfate–polyacrylamide gel electrophoresis (SDS–PAGE) and transferred onto Immobilon-P membranes (Millipore, Bedford, MA, USA). The transferred membranes were incubated with monoclonal anti-$p21^{WAF1}$ (Ab-1, Oncogene Research Products, Cambridge, MA, USA), monoclonal anti-p53 (DO-1, Oncogene Research Products), monoclonal anti-Noxa (ab13654, Abcom, Cambridge, UK), polyclonal anti-Bax (Cell Signaling, Beverly, MA, USA), polyclonal anti-caspase-3 (Calbiochem, San Diego, CA, USA), polyclonal anti-phosphorylated p53 at Ser-15 (Cell Signaling), polyclonal anti-NEDL1 or with polyclonal anti-actin (20–33, Sigma, St Louis, MO, USA) antibody followed by incubation with the appropriate HRP-conjugated secondary antibodies (Jackson ImmunoResearch Laboratories, West Grove, PA, USA). Bound antibodies were detected by ECL system (Amersham Biosciences, Piscataway, NJ, USA). For immunoprecipitation, 1 mg of protein was incubated with protein G-Sepharose beads (Amersham Biosciences). The precleaned lysates were incubated with polyclonal anti-NEDL1 antibody for 2 h at 4 °C and immunocomplexes were precipitated with protein G-Sepharose beads for additional 1 h at 4 °C. The immunocomplexes were washed three times with the lysis buffer, eluted from beads by adding 2 × SDS sample buffer, resolved by SDS–PAGE and subjected to immunoblotting with polyclonal anti-NEDL1 or with monoclonal anti-p53 (DO-1, Oncogene Research Products) antibody.

In vitro *binding assay*
Wild-type p53 and its deletion mutants were expressed *in vitro* using a T7 Quick Coupled Transcription/Translation System (Promega, Madison, WI, USA) in the presence of [^{35}S]methionine according to the manufacturer's recommendations. Cell lysates prepared from COS7 cells transfected with the expression plasmid encoding NEDL1 were mixed and incubated overnight at 4 °C. Reaction mixtures were then immunoprecipitated with the anti-NEDL1 antibody. Immunoprecipitates were washed extensively with the lysis buffer and resolved by SDS–PAGE. The gels were dried and subjected to autoradiography.

TUNEL assay
SH-SY5Y cells were grown on coverslips and treated with CDDP (20 μM). At the indicated time periods after the treatment with CDDP, cells were fixed in 4% paraformaldehyde and apoptotic cells were detected by using an *in situ* cell death detection Kit (Roche Molecular Biochemicals, Mannheim, Germany) according to the manufacturer's protocol. The coverslips were mounted with 4′,6-diamidino-2-phenylindole-containing mounting medium (Vector Laboratories, Burlingame, CA, USA) and observed under a Fluoview laser scanning confocal microscope (Olympus, Tokyo, Japan).

FACS analysis
U2OS and SAOS-2 cells were transfected with the expression plasmid for NEDL1. Forty-eight hours after transfection, floating and attached cells were collected, washed in phosphate-buffered saline and fixed in 70% ethanol at −20 °C. Following incubation in phosphate-buffered saline containing 40 μg ml^{-1} of propidium iodide and 200 μg ml^{-1} of RNase A for 1 h at room temperature in the dark, stained nuclei were analysed on a FACScan machine (Becton Dickingson, Mountain View, CA, USA).

RT–PCR
SH-SY5Y cells were treated with CDDP (20 μM). At the indicated time periods after the treatment, total RNA was prepared using an RNeasy mini kit (Qiagen, Valencia, CA, USA). Five micrograms of total RNA were employed to synthesize the first-strand cDNA by using random primers and SuperScript II reverse transcriptase (Invitrogen) according to the manufacturer's instructions. The resultant cDNA was subjected to the PCR-based amplification. The list of primer sets used will be provided upon request. The expression of glyceraldehyde-3-phosphate dehydrogenase was measured as an internal control. The PCR products were subjected to agarose gel electrophoresis and visualized by ethidium bromide staining.

Luciferase reporter assay
H1299 cells were allowed to adhere overnight in 12-well cell culture plates at a final density of 50 000 cells per well. Cells were then co-transfected with 25 ng of the p53 expression plasmid, 100 ng of the p53-responsible luciferase reporter construct (*$p21^{WAF1}$* or *Bax*) and 10 ng of pRL-TK *Renilla* luciferase cDNA together with or without increasing amounts of the NEDL1 expression plasmid (475 and 875 ng). Total amount of plasmid DNA per transfection was kept constant (1 μg) with an empty plasmid pcDNA3 (Invitrogen). Forty-eight hours after transfection, cells were lysed and both the firefly and *Renilla* luciferase activities were measured with dual-luciferase reporter assay system (Promega), according to the manufacturer's instructions. The firefly luminescence signal was normalized based on the *Renilla* luminescence signal.

Chromatin immunoprecipitation assay
Chromatin immunoprecipitation assay was performed according to the protocol provided by Upstate Biotechnology (Lake Placid, NY, USA). In brief, H1299 cells were transfected with the expression plasmid for p53 together with or without the expression plasmid for NEDL1. Forty-eight hours after transfection, cells were treated with 1% formaldehyde at 37 °C for 15 min. After being washed with ice-cold phosphate-buffered saline, cells were suspended with 200 μl of SDS lysis buffer (1% SDS, 10 mM EDTA and 50 mM Tris-HCl, pH 8.1) on ice for 10 min. Lysates were sonicated and insoluble materials were removed by centrifugation. Supernatants were then precleared with 20 μl of protein A agarose beads that had been preabsorbed with salmon sperm DNA at 37 °C for 30 min. The precleared chromatin solutions were immunoprecipitated with normal mouse serum or with anti-p53 antibody at 4 °C overnight, followed by incubation with 60 μl of protein A agarose beads for 1 h at 4 °C. Samples were eluted with 200 μl of the elution buffer (1% SDS and 0.1 M $NaHCO_3$) and then crosslinks were reversed by heating them at 65 °C for 6 h. Chromatin-associated proteins were digested with proteinase K at 45 °C for 1 h, and immunoprecipitated DNA was purified by using QIAquick PCR purification kit (Qiagen) according to the manufacturer's instructions. Purified DNA was analysed by PCR-based amplification. The primer set used to detect *$p21^{WAF1}$* promoter was as follows: 5′-CACCTTTCACCAT TCCCCTA-3′ (forward) and 5′-GCAGCCCAAGGACAAA ATAG-3′ (reverse).

Small interfering RNA
U2OS cells were transiently transfected with siRNA targeting NEDL1 (no. 1, 5′-CUAAAUGACUGGCGGAAUAUU-3′; no. 2, 5′-GAUGAGGUCUUGUCCGAAAUU-3′; no. 3, 5′-GAUGCCAGCUCGUACUUUGUU-3′; no. 4, 5′-CAGCU GCAAUUCCGAUUUGUU-3′) or control non-targeting

siRNA (Dharmacon, Chicago, IL, USA) by using Lipofect AMINE RNAiMAX transfection reagent (Invitrogen) according to the manufacturer's instructions. Forty-eight hours after transfection, total RNA was prepared and subjected to RT–PCR.

Colony formation assay

H1299, SH-SY5Y, U2OS and SAOS-2 cells were seeded at a final density of 1×10^5 cells per six-well dish and allowed to attach overnight. Cells were then co-transfected with the indicated combinations of the expression plasmids. Total amount of plasmid DNA per transfection was kept constant (2 μg) with pcDNA3. Forty-eight hours after transfection, cells were transferred to the fresh medium containing G418 (400 μg ml^{-1}). After 14 days, viable colonies were washed in phosphate-buffered saline and stained with Giemsa's solution.

Acknowledgements

We are grateful to Dr T Kamijo (Division of Biochemistry, Chiba Cancer Center Research Institute) for his helpful discussion. This work was supported in part by a grant-in-aid from the Ministry of Health, Labour and Welfare for Third Term Comprehensive Control Research for Cancer, a grant-in-aid for Scientific Research on Priority Areas from the Ministry of Education, Culture, Sports, Science and Technology, Japan, a grant-in-aid for Scientific Research from Japan Society for the Promotion of Science and Uehara Memorial Foundation.

References

Adhikary S, Marinoni F, Hock A, Hulleman E, Popov N, Beier R *et al.* (2005). The ubiquitin ligase HectH9 regulates transcriptional activation by Myc and is essential for tumor cell proliferation. *Cell* **123**: 409 421.

Bijur GN, De Sarno P, Jope RS. (2000). Glycogen synthase kinase-3beta facilitates staurosporine- and heat shock-induced apoptosis. *J Biol Chem* **275**: 7583 7590.

Cluskey S, Ramsden DB. (2001). Mechanisms of neurodegeneration in amyotrophic lateral sclerosis. *Mol Pathol* **54**: 386 392.

Cross DA, Culbert AA, Chalmers KA, Facci L, Skaper SD, Reith AD. (2001). Selective small-molecule inhibitors of glycogen synthase kinase-3 activity protect primary neurones from death. *J Neurochem* **77**: 94 102.

Di Lello P, Jenkins LM, Jones TN, Nguyen BD, Hara T, Yamaguchi H *et al.* (2006). Structure of the Tfb1/p53 complex: Insights into the interaction between the p62/Tfb1 subunit of TFIIH and the activation domain of p53. *Mol Cell* **22**: 731 740.

Donehower LA, Harvey M, Slagle BL, McArthur MJ, Montgomery Jr CA, Butel JS *et al.* (1992). Mice deficient for p53 are developmentally normal but susceptible to spontaneous tumours. *Nature* **356**: 215 221.

Ekegren T, Grundstrom E, Lindholm D, Aquilonius SM. (1999). Upregulation of Bax protein and increased DNA degradation in ALS spinal cord motor neurons. *Acta Neurol Scand* **100**: 317 321.

Gonzalez de Aguilar JL, Gordon JW, Rene F, de Tapia M, Lutz-Bucher B, Gaiddon C *et al.* (2000). Alteration of the Bcl-x/Bax ratio in a transgenic mouse model of amyotrophic lateral sclerosis: evidence for the implication of the p53 signaling pathway. *Neurobiol Dis* **7**: 406 415.

Hetman M, Cavanaugh JE, Kimelman D, Xia Z. (2000). Role of glycogen synthase kinase-3beta in neuronal apoptosis induced by trophic withdrawal. *J Neurosci* **20**: 2567 2574.

Hino S, Michiue T, Asashima M, Kikuchi A. (2003). Casein kinase I epsilon enhances the binding of Dvl-1 to Frat-1 and is essential for Wnt-3a-induced accumulation of beta-catenin. *J Biol Chem* **278**: 14066 14073.

Hollstein M, Sidransky D, Vogelstein B, Harris CC. (1991). p53 mutations in human cancers. *Science* **253**: 49 53.

Hupp TR, Lane DP. (1994). Regulation of the cryptic sequence-specific DNA-binding function of p53 by protein kinases. *Cold Spring Harb Symp Quant Biol* **59**: 195 206.

Kiryo-Seo S, Hirayama T, Kato R, Kiyama H. (2005). Noxa is a critical mediator of p53-dependent motor neuron death after nerve injury in adult mouse. *J Neurosci* **25**: 1442 1447.

Kishida M, Hino S, Michiue T, Yamamoto H, Kishida S, Fukui A *et al.* (2001). Synergistic activation of the Wnt signaling pathway by Dvl and casein kinase Iepsilon. *J Biol Chem* **276**: 33147 33155.

Kitanaka C, Kato K, Ijiri R, Sakurada K, Tomiyama A, Noguchi K *et al.* (2002). Increased Ras expression and caspase-independent neuroblastoma cell death: possible mechanism of spontaneous neuroblastoma regression. *J Natl Cancer Inst* **94**: 358 368.

Lee E, Salic A, Kirschner MW. (2001). Physiological regulation of [beta]- catenin stability by Tcf3 and CK1epsilon. *J Cell Biol* **154**: 983 993.

Levine AJ, Chang A, Dittmer D, Notterman DA, Silver A, Thorn K *et al.* (1994). The p53 tumor suppressor gene. *J Lab Clin Med* **123**: 817 823.

Martin LJ. (2000). p53 is abnormally elevated and active in the CNS of patients with amyotrophic lateral sclerosis. *Neurobiol Dis* **7**: 613 622.

Martin LJ, Liu Z. (2002). Injury-induced spinal motor neuron apoptosis is preceded by DNA single-strand breaks and is p53- and bax-dependent. *J Neurobiol* **5**: 181 197.

Miyazaki K, Fujita T, Ozaki T, Kato C, Kurose Y, Sakamoto M *et al.* (2004). NEDL1, a novel ubiquitin-protein isopeptide ligase for dishevelled-1, targets mutant superoxide dismutase-1. *J Biol Chem* **279**: 11327 11335.

Miyazaki K, Ozaki T, Kato C, Hanamoto T, Fujita T, Irino S *et al.* (2003). A novel HECT-type E3 ubiquitin ligase, NEDL2, stabilizes p73 and enhances its transcriptional activity. *Biochem Biophys Res Commun* **308**: 106 113.

Moll UM, LaQuaglia M, Benard J, Riou G. (1995). Wild-type p53 protein undergoes cytoplasmic sequestration in undifferentiated neuroblastomas but not in differentiated tumors. *Proc Natl Acad Sci USA* **92**: 4407 44011.

Nakagawara A, Ohira M. (2004). Comprehensive genomics linking between neural development and cancer: neuroblastoma as a model. *Cancer Lett* **204**: 213 224.

Pietenpol JA, Tokino T, Thiagalingam S, el-Deiry WS, Kinzler KW, Vogelstein B. (1994). Sequence-specific transcriptional activation is essential for growth suppression by p53. *Proc Natl Acad Sci USA* **91**: 1998 2002.

Roos WP, Kaina B. (2006). DNA damage-induced cell death by apoptosis. *Trends Mol Med* **12**: 440 450.

Shaw P, Freeman J, Bovey R, Iggo R. (1996). Regulation of specific DNA binding by p53: evidence for a role for *O*-glycosylation and charged residues at the carboxy-terminus. *Oncogene* **12**: 921 930.

Thomas MC, Chiang CM. (2005). E6 oncoprotein represses p53-dependent gene activation via inhibition of protein acetylation independently of inducing p53 degradation. *Mol Cell* **17**: 251 264.

Vousden KH, Lu X. (2002). Live or let die: the cell's response to p53. *Nat Rev Cancer* **2**: 594 604.

Watcharasit P, Bijur GN, Zmijewski JW, Song L, Zmijewska A, Chen X *et al.* (2002). Direct, activating interaction between glycogen synthase kinase-3beta and p53 after DNA damage. *Proc Natl Acad Sci USA* **99**: 7951 7955.

Supplementary Information accompanies the paper on the Oncogene website (http://www.nature.com/onc).

Biochemical and Biophysical Research Communications 370 (2008) 594–598

Contents lists available at ScienceDirect

Biochemical and Biophysical Research Communications

journal homepage: www.elsevier.com/locate/ybbrc

A newly identified dependence receptor UNC5H4 is induced during DNA damage-mediated apoptosis and transcriptional target of tumor suppressor p53

Hong Wang [a,b], Toshinori Ozaki [a,c], M. Shamim Hossain [a,c], Yohko Nakamura [a], Takehiko Kamijo [a], Xindong Xue [b], Akira Nakagawara [a,c,*]

[a] Division of Biochemistry, Chiba Cancer Center Research Institute, 666-2 Nitona, Chuoh-ku, Chiba 260-8717, Japan
[b] Department of Pediatric, Shengjing Hospital of China Medical University, Shenyang 110004, China
[c] Department of Molecular Biology and Oncology, Chiba University Graduate School of Medicine, Chiba 260-8717, Japan

ARTICLE INFO

Article history:
Received 26 March 2008
Available online 8 April 2008

Keywords:
Adriamycin
Apoptosis
DNA damage
p53
Transcription
UNC5H4

ABSTRACT

UNC5H4 is a netrin-1 receptor UNC5H family member. In this study, we found that *UNC5H4* is a direct transcriptional target of p53. During adriamycin (ADR)-mediated apoptosis, *UNC5H4* was significantly induced in *p53*-proficient U2OS cells but not in *p53*-deficient H1299 cells. Enforced expression of p53 induced *UNC5H4*. Consistent with these results, siRNA-mediated knockdown of p53 in U2OS cells attenuated ADR-dependent induction of *UNC5H4*. Indeed, we found four putative p53-responsive elements within intron 1 of *UNC5H4* gene. Luciferase reporter assay and ChIP analysis demonstrated that, among them, two tandem elements respond to exogenous p53 which is efficiently recruited onto them. Furthermore, enforced expression of UNC5H4 remarkably reduced number of drug-resistant colonies in *p53*-proficient cells but not in *p53*-deficient cells, suggesting that UNC5H4-induced apoptosis is dependent on *p53* status. siRNA-mediated knockdown of UNC5H4 rendered U2OS cells resistant to ADR. Collectively, our present results suggest that UNC5H4 amplifies p53-dependent apoptotic response.

© 2008 Elsevier Inc. All rights reserved.

Type I transmembrane receptors such as DCC (deleted in colorectal cancer) and UNC5H have been considered to belong to the so-called dependence receptor family [1,2]. These receptors share functional similarity to promote apoptosis without their respective ligands including netrin family, but inhibit apoptosis when bound to these ligands [3]. As described [1], DCC was one of caspase substrates and served as a caspase amplifier under conditions in which the ligand is unavailable. Extensive studies suggested that DCC acts as a tumor suppressor [4], however, *DCC* is rarely mutated in human cancers [5]. Mammalian UNC5H family is composed of UNC5H1–4 [6–8]. Among them, UNC5H4 has been recently found in human genome database [9]. Thiebault et al. described that expression levels of *UNC5H1–3* are strongly down-regulated in various primary tumors which is associated with loss of heterozygosity (LOH) within *UNC5H* loci and enforced expression of UNC5H1, UNC5H2 or UNC5H3 inhibits malignant transformation, which is related to their pro-apoptotic activity [10]. According to their results, UNC5H-mediated apoptosis was dependent on their cytoplasmic death domain and potent caspase inhibitor abrogated their pro-apoptotic activity. Consistent with these observations, UNC5H1–3 contained classic caspase cleavage site (DXXD) [11] and caspase-mediated cleavage of UNC5H was required for cell death induction [2]. Although UNC5H family has pro-apoptotic activity [12], the precise molecular mechanisms behind UNC5H-mediated apoptosis remained unclear.

Of note, *UNC5H2* is a direct transcriptional target of p53 and UNC5H2-mediated apoptosis is regulated in a p53-dependent manner [13]. Based on their results, netrin-1 inhibited p53-dependent apoptosis without affecting expression levels of p53. Alternatively, Llambi et al. found that UNC5H2 interacts with death-associated protein kinase (DAP-kinase) and their interaction enhances catalytic activity of DAP-kinase [14]. Intriguingly, DAP-kinase required functional p53 for induction of apoptosis [15]. In contrast to UNC5H1–3, little is known about functional significance of UNC5H4. In the present study, we found that *UNC5H4* is a direct transcriptional target of p53 and UNC5H4-mediated apoptosis is dependent on *p53* status.

Materials and methods

Cell lines and culture. Human osteosarcoma U2OS and SAOS-2 cells were maintained in Dulbecco's modified Eagle's medium (DMEM) supplemented with 10% heat-inactivated fetal bovine serum (FBS, Invitrogen), penicillin (50 U/ml) and streptomycin (50 μg/ml). Human lung carcinoma H1299 cells were cultured in RPMI 1640 medium supplemented with 10% heat-inactivated FBS and antibiotic mixture. Cells were grown at 37 °C in a humidified atmosphere of 5% CO_2 in the air. Where indicated, cells were exposed to adriamycin (ADR) at a final concentration of 1 μM.

* Corresponding author. Address: Division of Biochemistry, Chiba Cancer Center Research Institute, 666-2 Nitona, Chuoh-ku, Chiba 260-8717, Japan. Fax: +81 43 265 4459.
E-mail address: akiranak@chiba-cc.jp (A. Nakagawara).

0006-291X/$ - see front matter © 2008 Elsevier Inc. All rights reserved.
doi:10.1016/j.bbrc.2008.03.152

Transfection. Cells were transfected with the indicated expression plasmids using LipofectAMINE 2000 transfection reagent (Invitrogen) according to the manufacturer's instructions.

Cell survival assay. Cells were seeded at a density of 5×10^3 cells/96-well cell culture plates and allowed to attach overnight. Cells were then treated with 1 μM of ADR. At the indicated time points after ADR treatment, 10 μl of a modified 3-(4,5-dimethylthiazol-2-yl) 2,5-diphenyl-tetrazolium bromide solution (Dojindo) were added to the culture and reaction mixtures were incubated at 37 °C for 1 h. The absorbance readings for each well were carried out at 570 nm using the microplate reader (Model 450, Bio-Rad Laboratories).

RT-PCR. Total RNA was isolated from the indicated cells by using RNeasy Mini Kit (Qiagen) according to the manufacturer's recommendations and reverse transcribed in the presence of random primers and SuperScript II reverse transcriptase (Invitrogen). The resultant first-strand cDNA was amplified by PCR to measure expression levels of genes of interest. The oligonucleotide primers used in this study were as follows: *p53*, 5′-ATTTGATGCTGTCCCCGGACGATATTGAAC-3′ (sense) and 5′-ACCCTTTTTGGACTTCAGGTGGCTGGAGTG-3′ (antisense); *p21*^{WAF1}, 5′-ATGAAATT CACCCCCTTTCC-3′ (sense) and 5′-CCCTAGGCTGTGCTCACTTC-3′ (antisense); *Bax*, 5′-TTTGCTTCAGGGTTTCATCC-3′ (sense) and 5′-CAGTTGAAGTTGCCGTCAGA-3′ (antisense); *UNC5H4*, 5′-TGAACTGCAGATGCCATAGG-3′ (sense) and 5′-GGTTTCAGG GACACTGTGGT-3′ (antisense); *GAPDH*, 5′-ACCTGACCTGCCGTCTAGAA-3′ (sense) and 5′-TCCACCACCCTGTTGCTGTA-3′ (antisense). PCR products were separated by 1.5% agarose gel electrophoresis and visualized by ethidium bromide staining.

Immunoblotting. Cells were washed in ice-cold phosphate-buffered saline (PBS) and lysed in SDS-sample buffer containing 10% glycerol, 5% β-mercaptoethanol, 2.3% SDS and 62.5 mM Tris–HCl (pH 6.8). The protein concentration of cell lysates was determined by using Bio-Rad protein assay dye reagent (Bio-Rad Laboratories) according to the manufacturer's instructions. Bovine serum albumin (BSA) was used as a standard. Equal amounts of cell lysates were separated by 10% SDS–polyacrylamide gel electrophoresis, electro-transferred onto Immobilon-P membrane filters (Millipore) and blocked with 0.3% non-fat milk in Tris-buffered saline (TBS) containing 0.1% Tween 20 at 4 °C. The membranes were probed with monoclonal anti-p53 (DO-1: Oncogene Research Products), polyclonal anti-phospho-p53 at Ser-15 (Cell Signaling Technology), polyclonal anti-p21^{WAF1} (H-164, Santa Cruz Biotechnology), polyclonal anti-PARP (Cell Signaling Technology) or with anti-actin (20-33: Sigma) antibody at room temperature for 1 h followed by incubation with horseradish peroxidase-conjugated secondary antibodies (Cell Signaling Technology) at room temperature for 1 h. Immunoreactive bands were visualized by using ECL system (Amersham Biosciences) according to the manufacturer's instructions.

Establishment of p53-knocked down cell clones. U2OS cells were transfected with the empty plasmid (pSUPER, OligoEngine) or with the expression plasmid for siRNA against p53 (pSUPER-p53). Forty-eight hours after transfection, cells were transferred into the fresh medium containing G418 (Sigma) at a final concentration of 500 μg/ml and incubated for two weeks. Then, G418-resistant clones were picked up and cultured in the presence of G418. Expression levels of p53 in each cell clone were analyzed by immunoblotting.

Construction of luciferase reporter plasmids. The indicated luciferase reporter constructs driven by putative p53-responsive elements of *UNC5H4* gene were generated by using the following primer sets: RE1, 5′-GAGCTCATGTTGGCCAGGCTAGTC-3′ (sense) and 5′-GTGCTCACAGGGCAATGACTCACCTC-3′ (antisense); RE2, 5′-GGTACCT CATCCTCTGAACGTTAAC-3′ (sense) and 5′-GGTACCTAAAGGGACTAGATCATG-3′ (antisense); RE3, 5′-GAGCTCTCAGATTGCATGTCTGTAC-3′ (sense) and 5′-GAGCTCAGC CTCACATAACACAGAGT-3′ (antisense); RE4, 5′-GAGCTCTAGGGCAGTTAATCTTGC-3′ (sense) and 5′-GAGCTCACCTATGAAATGGTGGAG-3′ (antisense). The resultant PCR products were gel-purified and inserted into appropriate restriction sites of pGL3-promoter plasmid (Promega) to give p53-RE1, p53-RE2, p53-RE3 and p53-RE4. The constructs were verified by DNA sequencing (Applied Biosystems).

Luciferase reporter assay. p53-deficient H1299 cells were seeded at a density of 5×10^4 cells/12-well cell culture plates and allowed to attach overnight. Cells were transiently co-transfected with 100 ng of pGL3-promoter plasmid (Promega), p53-RE1, p53-RE2, p53-RE3 or p53-RE4, 10 ng of *Renilla* luciferase reporter construct (pRL-TK, Promega) and 25 ng of the expression plasmid for FLAG-p53. Total amount of plasmid DNA per transfection was kept constant (510 ng) with pcDNA3. Forty-eight hours after transfection, cells were lysed and their luciferase activities were measured by using Dual-Luciferase Assay System (Promega) according to the manufacturer's instructions. The firefly luminescence signal was normalized based on the *Renilla* luminescence signal.

Chromatin immunoprecipitation (ChIP) assay. ChIP assay was performed as described [16]. In brief, H1299 cells were transfected with the empty plasmid or with the expression plasmid for p53. Forty-eight hours after transfection, cells were cross-linked with 1% formaldehyde in medium for 10 min at 37 °C. Cross-linked chromatin was prepared from cells and sonicated to an average length of 200–800 nucleotides, precleaned with salmon sperm DNA/protein A-agarose beads and immunoprecipitated with normal mouse serum (NMS) or with monoclonal anti-p53 antibody. The immunoprecipitates were eluted with 100 μl of elution buffer (1% SDS and 1 mM $NaHCO_3$). Formaldehyde-mediated cross-links were reversed by heating at 65 °C for 4 h and the reaction mixtures were treated with proteinase K at 45 °C for 1 h. Genomic DNA was purified using the QIAquick PCR purification kit (Qiagen). Purified DNA was amplified by PCR using the following primer sets: RE1, 5′-GAGCTCATGTTGGCCAGGCTAGTC-3′ (sense) and 5′-GTGCTCACAGGGCAATGACT CACCTC-3′ (antisense); RE2, 5′-GGTACCTCATCCTCTGAACGTTAAC-3′ (sense) and 5′-GGTACCTAAAGGGACTAGATCATG-3′ (antisense); RE3, 5′-TCAGATTGCATGTCTG TAC-3′ (sense) and 5′-AGCCTCACATAACACAGAGT-3′ (antisense).

Colony formation assay. U2OS and H1299 cells were transfected with the empty plasmid (pcDNA3) or with the expression plasmid encoding UNC5H4. Forty-eight hours after transfection, cells were transferred into fresh medium supplemented with G418 (400 μg/ml). After two weeks of selection, drug-resistant colonies were stained with Giemsa's solution and number of drug-resistant colonies was scored.

siRNA-mediated knockdown of UNC5H4. SAOS-2 cells were transfected with 10 nM of control siRNA or with siRNA against UNC5H4 (Dharmacon) by using LipofectAMINE RNAiMAX (Invitrogen) according to the manufacturer's recommendations. A list of siRNA sequences used will be provided upon request. Forty-eight hours after transfection, total RNA was prepared and analyzed for expression levels of *UNC5H4* by RT-PCR.

Flow cytometry. Forty-eight hours after the treatment with ADR (1 μM), floating and attached cells were collected, washed in ice-cold PBS and fixed in 70% ethanol at −20 °C. The cells were washed in ice-cold PBS and resuspended in phosphate-citrate buffer (4 mM citric acid and 200 mM Na_2HPO_4) and kept at room temperature for 15 min. Nuclear DNA was stained with propidium iodide (40 μg/ml) in the presence of RNase A (10 μg/ml) and the reaction mixture was incubated in the dark for 30 min. After the incubation with propidium iodide, DNA content of cells was examined by FACScan flow cytometer (Beckton Dickinson) using CellQuest software.

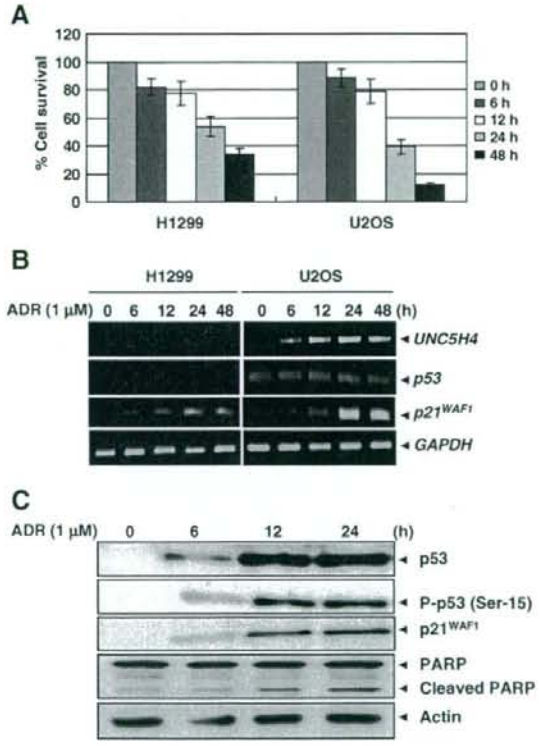

Fig. 1. Transcriptional activation of *UNC5H4* in *p53*-proficient cells but not in *p53*-deficient cells exposed to DNA damage. (A) Cell survival assays. p53-deficient H1299 cells and *p53*-proficient U2OS cells were treated with 1 μM of ADR. At the indicated time points, cell viability was examined by MTT assay. (B) RT-PCR. At the indicated time points after ADR treatment (1 μM), total RNA was prepared from H1299 (left panels) and U2OS (right panels) cells and analyzed for expression levels of *UNC5H4*, *p53* and *p21*^{WAF1}. Amplification of *GAPDH* was used as an internal control. (C) Immunoblotting. U2OS cells were exposed to ADR (1 μM). At the indicated time points, cell lysates were prepared and subjected to immunoblotting with the indicated antibodies. Immunoblotting for actin is shown as a loading control.

Results

DNA damage-induced up-regulation of UNC5H4

To examine expression patterns of *UNC5H4* and *p53*-related genes in response to DNA damage, *p53*-deficient lung carcinoma H1299 and *p53*-proficient osteosarcoma U2OS cells were exposed to 1 μM of adriamycin (ADR). Both cells underwent apoptosis as examined by MTT assay (Fig. 1A). Similar results were also obtained by FACS analysis (data not shown). During ADR-mediated apoptosis, $p21^{WAF1}$ which is one of p53-target genes [17] and *UNC5H4* were strongly induced in U2OS cells (Fig. 2B). Similar results were also obtained in neuroblastoma SH-SY5Y cells bearing wild-type *p53* (data not shown). In contrast, *UNC5H4* was undetectable in H1299 cells exposed to ADR, however, ADR-mediated up-regulation of $p21^{WAF1}$ was detectable, which might be due to the induction of another p53 family member p73 (data not shown). Immunoblot analysis revealed that ADR treatment results in a remarkable accumulation of p53, phospho-p53 at Ser-15, cleaved PARP and $p21^{WAF1}$ in U2OS cells (Fig. 1C).

UNC5H4 is a transcriptional target of p53

These observations prompted us to examine whether *UNC5H4* could be a transcriptional target of p53. To address this issue, H1299 cells were transfected with the expression plasmid encoding p53. Time course experiments demonstrated that p53 induces expressions of *UNC5H4*, $p21^{WAF1}$ and *Bax* [18] in a time-dependent manner (Fig. 2A). Transfection with the empty plasmid alone had undetectable effect on *UNC5H4* (data not shown). To further confirm this notion, we established two stable U2OS transfectants in which p53 was knocked down (N-1 and N-2) and one control transfectant (C-1). These transfectants were then treated with ADR and analyzed for expression levels of *UNC5H4*. As seen in Fig. 2B, p53 was successfully knocked down and ADR-mediated induction of p53 and $p21^{WAF1}$ were undetectable in N-1 and N-2 cell clones. ADR-mediated up-regulation of p53 and $p21^{WAF1}$ were observed in C-1 cell clone. ADR treatment significantly induced expression of *UNC5H4* in C-1 cell clone, whereas exposure to ADR had undetectable effect on *UNC5H4* in N-1 and N-2 cell clones, suggesting that *UNC5H4* is a transcriptional target of p53 and also involved in DNA damage response.

p53 enhances the promoter activity of UNC5H4 gene

It has been shown that *UNC5H2* composed of 17 exons is mapped at chromosome 10 and two functional p53-binding sequences are detectable within intron 1 of *UNC5H2* [13]. During extensive search for putative p53-responsive element(s) within intron 1 of *UNC5H4* gene, we identified four candidate p53-responsive elements (p53-RE1-4). To verify whether these elements could respond to p53, each of these elements was subcloned upstream of pGL3-promoter plasmid and luciferase reporter assays

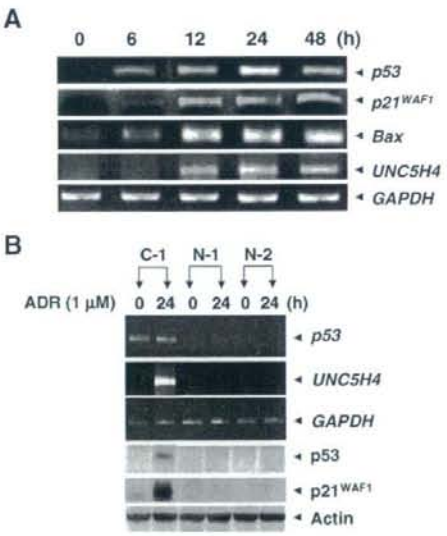

Fig. 2. p53-mediated transcriptional activation of *UNC5H4*. (A) Time course experiments. H1299 cells were transfected with the expression plasmid encoding p53. At the indicated time points, total RNA was prepared and analyzed for expression levels of *p53*, $p21^{WAF1}$, *Bax* and *UNC5H4* by RT-PCR. (B) siRNA-mediated knockdown of p53 attenuates ADR-dependent up-regulation of *UNC5H4*. U2OS cells were transfected with the empty plasmid or with the expression plasmid for siRNA against p53. Forty-eight hours after transfection, cells were transferred into fresh medium containing G418 (500 μg/ml) and maintained for two weeks. We then established control (C-1) and knockdown transfectants (N-1 and N-2). These stable transfectants were treated with 1 μM of ADR. Twenty-four hours after the exposure to ADR, total RNA and cell lysates were prepared and subjected to RT-PCR (upper panels) and immunoblotting (lower panels), respectively.

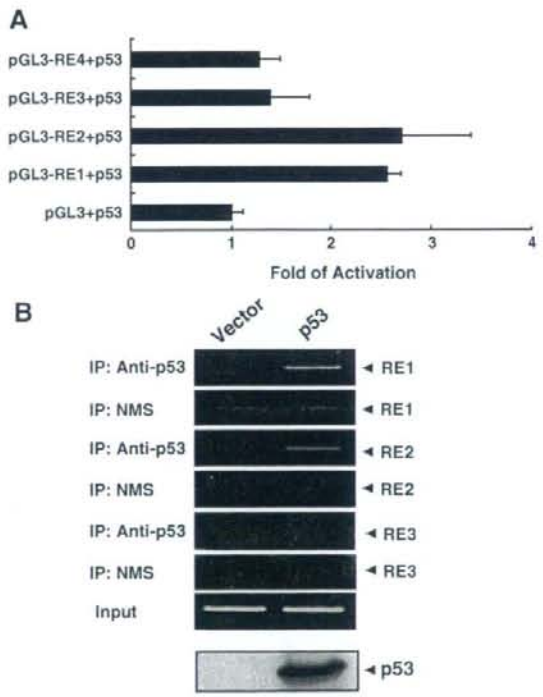

Fig. 3. *UNC5H4* is a direct target of p53. (A) Luciferase reporter assay. H1299 cells were co-transfected with 100 ng of the indicated luciferase reporter plasmids, 10 ng of *Renilla* luciferase reporter and 25 ng of expression plasmid for p53. Total amount of plasmid DNA per each transfection was kept constant (510 ng) with pcDNA3. All transfections were carried out in triplicate. Forty-eight hours after transfection, cells were lysed and their luciferase activities were measured by Dual-Luciferase Assay System. The firefly luciferase activity was normalized based on *Renilla* luciferase activity. Graphs indicate the average of three independent experiments. (B) ChIP assay. Cross-linked chromatin was prepared from H1299 cells transfected with the empty plasmid or with the expression plasmid for p53, sonicated to an average length of 200–800 nucleotides and immunoprecipitated with normal mouse serum (NMS) or with monoclonal anti-p53 antibody. Precipitated genomic DNA was amplified by PCR using the indicated primer sets (upper panels). Lower panel shows the expression of exogenous p53 as examined by immunoblotting.